Parametric optimization and performance analysis of Geothermal oraganic Rankine cycle using zeotropic mixture of R600a/DME as working fluid

A Major Thesis submitted in the partial fulfilment of the requirement for the award of Degree of

Master of Technology
In
Renewable Energy Technology

Submitted by:
Shubham Pandey
(2K14/RET/16)

Under the guidance of:
Dr. Akhilesh Arora

Department Of Mechanical Engineering and Production & Industrial Engineering
DELHI TECHNOLOGICAL UNIVERSITY
Shahbad, Daulatpur,Main Bawana Road, Delhi – 42

CANDIDATE'S DECLARATION

I hereby declare that the work which being presented in the major thesis entitled "**Parametric optimization and performance analysis of geothermal organic rankine cycle using zeotropic mixture of R600a/DME as working fluid**" in the partial fulfilment for the award of the degree of Master of Technology in "RENEWABLE ENERGY TECHNOLOGY" submitted to Delhi Technological University (Formerly Delhi College of Engineering), is an authentic record of my own work carried out under the supervision of Dr. Akhilesh Arora, Department of Mechanical Engineering, Delhi Technological University (Formerly Delhi College of Engineering). I have not submitted the matter of this dissertation for the award of any other Degree or Diploma or any other purpose what so ever. I confirm that I have read and understood 'Plagiarism policy of DTU'. I have not committed plagiarism when completing the attached piece of work, similarity found after checking is 0%.

SHUBHAM PANDEY
Roll No. 2k14/RET/16
Place: Delhi
Date:

CERTIFICATE

This is to certify that the above statement made by SHUBHAM PANDEY is true to the best of my knowledge and belief.

DR. AKHILESH ARORA
Assistance Professor
Department of Mechanical Engineering
Delhi Technological University
(Formerly Delhi College of Engineering)
Delhi-110042

ACKNOWLEDGMENT

It is a great pleasure to have the opportunity to extent my heartiest felt gratitude to everybody who helped me throughout the project.

It is distinct pleasure to express my deep sense of gratitude and indebtedness to my learned supervisor **Dr. AKHILESH ARORA**, Assistant Professor in Mechanical Department, Delhi Technological University (Formerly Delhi College of Engineering), for his invaluable guidance, encouragement and patient review. His continues inspiration only has made me complete this dissertation.

I would also like to take this opportunity to present my sincere regards to **Dr. R S MISHRA**, Head of Department, Mechanical Department, Delhi Technological University (Formerly Delhi College of Engineering), for his kind support and encouragement.

I am thankful to my friends and classmates for their unconditional support and motivation for this dissertation.

SHUBHAM PANDEY
Roll No. 2k14/RET/16

ABSTRACT

Organic Rankine cycle is preferred to convert low temperature geothermal energy to electricity. The working fluid selection and system parameters optimisation are the main approaches to improve the performance of ORC system. Zeotropic mixtures are showing promise as ORC working fluids due to better match between the working fluid and the heat source/sink temperatures.

This study optimises the evaporator inlet temperature of mixture (R600a/DME) for various mass fractions to maximize the net work output and compare the thermal efficiency and exergetic efficiency of system for geothermal water temperature of 393K. Irreversibility in each component of system and mass flow rate of mixture are also found in this analysis by varying mass fraction of R600a. After doing analysis, it was found that R600a/DME (0.8/0.2) gives the maximum net work output corresponding to 343K inlet temperature to evaporator. Among all selected proportions, R600a/DME (0.6/0.4) has both maximum thermal efficiency and maximum exergetic efficiency corresponding to 373k inlet temperature to evaporator. Irreversibility present in evaporator is minimum for mass fraction 0.6 of R600a. Mass flow rate of mixture increases with mass fraction of R600a upto 0.6 and then become approximately constant.

TABLE OF CONTENT

NOMENCLATURE

h	Specific enthalpy (kJ/kg)
S	Specific entropy (kJ/kgK)
$\dot{m}$	Mass flow rate (kg/s)
P	Pressure (kpa)
T	Temperature (K)
Q	Heat transfer (kW)
W	Work transfer (kW)
İ	Irreversibility rate (kW)
H	Isentropic efficiency
η_{th}	Thermal efficiency
η_{ex}	Exergetic efficiency
C	Specific heat (kJ/kgK)

Subscript/Superscript

T_e	Evaporator temperature
T_c	Condenser temperature
P_e	Evaporator pressure
P_c	Condenser pressure
T_{pp}	Pinch point temperature
evp	Evaporator
con	Condenser
turb	Turbine

LIST OF FIGURES

LIST OF TABLES

CHAPTER-1
INTRODUCTION

1.1 MOTIVATION

With the cost of energy constantly increasing and the entire world turning towards being more environmentally friendly and more energy efficient there is a need for more alternative and renewable sources of energy. One of these sources is an organic Rankine cycle (ORC). ORC converts low temperature waste heat into electricity and emits absolutely no carbon dioxide or pollutants. ORC falls under the category of micro turbines which mean that if a facility implements an ORC they are able to file for certain tax breaks and incentives from the state and federal government that can make the purchase and implementation of ORC's easier and cheaper for the facilities that are installing them. Although these cycles are only approx 10% to 15% efficient they are utilizing energy from exhaust gases which is otherwise wasted and expelled into the atmosphere. Therefore they are essentially creating free energy and have the potential to save companies that install these cycles hundreds of thousands of dollars.

1.2 HISTORY

A Rankine cycle is the basic power production cycle used in about 80% of the electricity produced worldwide. The cycle is first accredited to, and named after, William John Macquorn Rankine a famous Scottish engineer and physicist. William Rankine first developed the, soon to be named, Rankine cycle after studying and developing the theory of heat engines in the early 1850's. The first publication of a Rankine cycle was in a published work by William Rankine in 1859. The basic Rankine cycle is a closed loop process that takes a working fluid and pumps the fluid through a boiler until it is changes phase and becomes a vapour, the vapour is then forced through a turbine which rotates a shaft that is connected to a generator that produces electricity, the vapour is then pushed through a condenser where the vapour is fully condensed to a liquid, the liquid then enters a pump and starts the cycle again. In the basic Rankine cycle the working fluid is water which is easily converted to steam in the boiler and can be used to generate electricity or can be used in a steam engine [1]. The basic Rankine cycle setup and its temperature entropy diagram can be seen in fig.1.1 and fig.1.2.

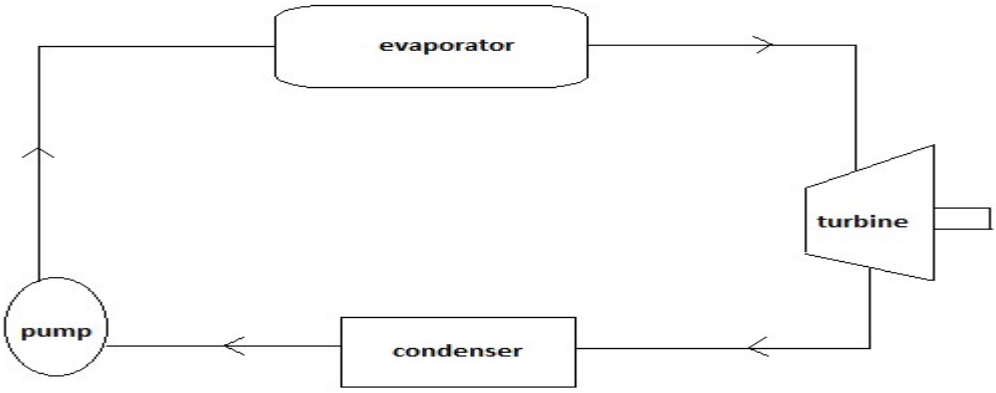

Fig.1.1 Schematic diagram of basic Rankine cycle

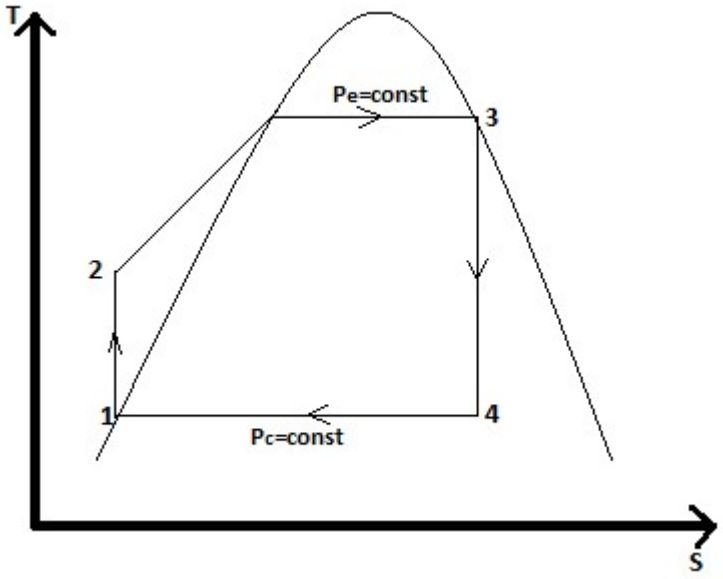

Fig.1.2 T-S diagram of basic Rankine cycle

1.3 ORGANIC RANKINE CYCLE

An organic Rankine cycle is similar to Rankine cycle that utilizes an organic based fluid as the working fluid. An organic fluid is defined as a fluid that contains carbon. The main types of organic fluids are refrigerants or hydrocarbon chain fluids. The first organic Rankine cycle was developed by Israeli solar engineer, Harry Zvi Tabor [1]. He originally started the Israeli Solar Engineering project in the late 1950's. He realized that low-grade heat was available from the sun and that he could convert this heat to electricity for use in rural areas that were unable to connect to the electrical grid directly.

He first looked at using a reciprocating engine but decided that there were too many moving parts and many maintenance issues for a very rural application so he decided to design the first organic Rankine cycle, which could utilize the low temperature waste heat and only had one moving part in the turbine. The first organic Rankine cycle was designed in 1961 and was displayed in the United Nations conference on New Sources of energy in Rome. The prototype was a three-kilowatt system and did not get widely produced after its premier [2].

An organic Rankine cycle is a basic power production cycle that utilizes low temperature waste heat to produce electricity. An organic Rankine cycle is similar to a Rankine cycle in the sense that it turns a fluid to a vapour and forces the vapour through a turbine which spins a shaft connected to a generator which in turn produces electricity. The vapour is then forced through a condenser that changes the vapour back to a liquid which then enters a pump and starts the cycle again. An organic Rankine cycle is different from a Rankine cycle because it uses a fluid that is organic based, meaning it contains carbon, and has a lower boiling point. Since the fluid has a lower boiling point the cycle can utilize lower temperature heat to cause the fluid to change phase from a liquid to a vapour.

1.4 APPLICATIONS

Geothermal energy is thermal energy generated and stored in the Earth. Thermal energy is the energy that determines the temperature of matter. The geothermal energy of the Earth's crust originates from the original formation of the planet and from radioactive decay of materials (in currently uncertain but possibly roughly equal proportions). The geothermal gradient, which is the difference in temperature between the core of the planet and its surface, drives a continuous conduction of thermal energy in the form of heat from the core to the surface.

A very large amount of geothermal energy is stored in the earth, but 70% of the geothermal source is low-enthalpy geothermal water at temperatures lower than 150°C. The International Geothermal Association (IGA) has reported that 10,715 megawatts (MW) of geothermal power in 24 countries is online, which was expected to generate 67,246 GWh of electricity in 2010. This represents a 20% increase in online capacity since 2005. IGA projects growth to

18,500 MW by 2015, due to the projects presently under consideration, often in areas previously assumed to have little exploitable resource [3].

Organic Rankine cycle (ORC) systems have been developed to convert low-enthalpy geothermal energy to electricity, but the thermal efficiencies of the geothermal ORC systems are generally less than 12%. The working fluid selection and system parameters have been optimized in various studies to improve the thermal efficiencies of geothermal ORC systems. A zeotropic mixture can better match the temperature profiles during evaporation and condensation due to the temperature glides with the changing component concentrations in each phase of the mixture. Therefore, the use of zeotropic mixtures as ORC working fluids has received more attention recently [4].

The thermal efficiency of geothermal electric plants is low, around 10 to 23%, because geothermal fluids do not reach the high temperatures of steam from boilers. The laws of thermodynamics limit the efficiency of heat engines in extracting useful energy. Exhaust heat is wasted, unless it can be used directly and locally, for example in greenhouses, timber mills, and district heating. System efficiency does not materially affect operational costs as it would for plants that use fuel, but it does affect return on the capital used to build the plant.

Solar thermal applications are also a big field for ORC's because the solar thermal system is already producing hot water which means there are no extra costs for heat exchangers and the water can be pumped directly into the ORC. Advantages to the solar thermal applications are that if a facility uses a lot of hot water a system can be oversized for the facility's need and the extra hot water can be used to run an ORC, which means the incentives are doubled since now the facility is implementing a solar thermal system and a micro turbine system.

The application of prime movers is the least likely area for implementation because most large vehicles such as barges or trains do not have a large enough flow rate to support and ORC. Prime movers are also an unlikely choice for ORC's because the exhaust is intermittent and dependent on the use of the vehicle. ORC's can also be implemented in biomass plants that are exhausting directly to the atmosphere. ORC plants like this currently exist in Germany. The most common implementation of an ORC is in the solar thermal field, due to the free heating of water from the

sun. The main issue with this application is that the system needs to remain pressurized so the water does not turn to steam before it enters the ORC [3].

1.5 GEOTHERMAL ENERGY IN INDIA

Several geothermal provinces in India categorized by high heat flow (78.468 MW/m^2) and thermal gradients (47100^oC/km) discharge about 450 thermal springs. After the oil crisis in 1970s, the Geological Survey of India conducted reconnoitres survey on them in collaboration with UN organization and reported the results in several of their records and special publications. Subsequently, detailed geological, geophysical and tectonic studies on several thermal provinces [5]. Geochemical characteristics of the thermal discharges and reservoir temperature estimations have been carried out by several workers [6]. These investigations have identified several sites which are suitable for power generations well as for direct use. These provinces are capable of generating 10,600 MW of power. Though geothermal power production in Asian countries like Indonesia, Philippines has gone up by 1800 MW in 1998, India with its 10,600 MW geothermal power potential is yet appear on the geothermal power map of the world. Availability of large recoverable coal reserves and a powerful coal lobby is preventing healthier growth of nonconventional energy sector, including geothermal. However, with the growing environmental problems associated with thermal power plants, future for geothermal power in India appears to be bright. Several IPPs engaged in nonconventional energy projects are frantically searching for foreign financial institutions to develop geothermal based energy sources.

CHAPTER-2

LITERATURE REVIEW

2.1 Summarization of various authors work

Many journal articles and research papers were read and studied in order to determine research that had already been performed in the field of geothermal organic Rankine cycle technology using zeotropic mixtures.

Angelino and Paliano [4] examined the performance of a geothermal ORC with mixtures of n-butane and n-hexane. Their results showed that the ORC with a mixture of n-butane and n-hexane produced 6.8% more electricity than with just n-pentane.

Heberle et al. [7] investigated the exergy efficiency of subcritical ORCs with zeotropic mixtures (isobutane/isopentane and R227ea/R245fa) as the working fluids for conversion of low-enthalpy geothermal sources. Their results showed that the exergy efficiencies increased by 4.3–15% using mixtures compared to the most efficient pure fluid for geothermal source temperatures below 120℃. They pointed out that the temperature glide during condensation should be fit to the cooling water temperature difference.

Baik et al. [8] investigated the power enhancement potential of a transcritical ORC with R125 based HFC mixture working fluids using a low-temperature geothermal heat source of about 100℃. Their results showed that the optimized transcritical ORC with an R125/R245fa mixture working fluid yielded 11% more power than the optimized subcritical ORC with just R134a.

Liu et al. [9] investigated the method to determine the mixture condensation pressure and the effect of the condensation temperature glide on the geothermal ORCs performance with zeotropic mixtures as working fluids. Their results showed two maxima in the cycle thermal efficiency, exergy efficiency and net power output when the condensation temperature glide matches the cooling water temperature rise. Use of zeotropic mixtures can also increase the thermodynamic performance of ORCs driven by solar energy or high temperature heat sources.

Papadopoulos et al. [10] proposed a holistic approach for fluid selection. By the use of computer aided molecular design in conjunction with process optimization physical, chemical, environmental, safety and economic properties of pure ORC fluids were evaluated. Schuster et al. considered different working fluids in supercritical cycles.

Demuth [11] evaluated in a case study for a geothermal power plant two-component mixtures of natural hydrocarbons for certain compositions at 137℃ and 182℃ geothermal water temperatures. For subcritical cycles efficiency increases up to 14% compared to the most efficient pure fluid propane.

Heberle and Brüggemann [12] investigated both series and parallel CHP system configurations for thermal utility temperature up to 90℃. Their analysis showed higher second law efficiency for the CHP series concept. They reported an increase of 20% in second law efficiency of the CHP system when compared to the stand-alone power generation ORC. The system's second law efficiency reached about 54% for the 'series' concept and about 50% for the 'parallel' concept.

Kim et al. [13] analyzed the performances with seven different fluids of a regenerative ORC with heat supplied in series driven by a low-temperature heat source. They found that higher turbine inlet pressure leads to lower second law efficiency of ORC, but anyway higher than the CHP system. Also the optimal working fluids vary with the heat source temperature.

Gozdur and Nowak [14] studied Rankine cycles with heat source temperature of 80℃ to 115℃ using natural and synthetic working fluids, as well as mixtures. They found that highest values of power obtained have been for the natural working fluid-propylene and single component synthetic fluid R227ea; highest values of efficiency obtained have been for the natural working fluid-propylene and single-component synthetic fluid R245fa.

Habka and Ajib [15] investigated the effect of the heating demand parameters of the cogenerative section on the overall power plant behavior for two connections of CHP systems (parallel plant and CHP integration according to NueStadt Glewe plant in Germany) operating with R134a and fuelled by a geothermal resource at 100℃. They investigated the exergy

efficiency, net output power of ORC, irreversibility related to the exhausted geothermal water and the total heat exchangers surface areas. They concluded that the performances of such CHP configurations are compromised when working at high cogeneration heating parameters (i.e. temperature and heat demand of the utilities). They also found that the parallel connection is more economical and that the series connection is energetically more efficient and that, on the contrary, the integration according to NueStadt Glewe power plant does not provide any significant optimization. They also noticed that the maximum optimized mechanical power in all of the investigated CHP configurations is not higher than 50% of the maximum power produced by the corresponding stand-alone ORC.

Guo et al. [16] investigated a novel cogeneration system consisting of low temperature geothermal-powered ORC, an intermediate heat exchanger and a heat pump subsystem at same time identifying a suitable working fluid. The results indicated that the optimized fluids based on each screening criteria are not the same and there exist optimum evaporation temperatures maximizing the P_{net} value and minimizing the $A/P_{net.}$

Hung et al. [17] studied an ORC using different fluids among wet, dry and isentropic fluids. Dry and isentropic fluids showed better thermal efficiencies and moreover, they did not condense during expansion in the turbine thus less damage in the machine was obtained.

Tchanche et al. [18] analyzed thermodynamic characteristics and performances of 20 fluids in a low-temperature solar organic Rankine cycle and R134a was recommended.

Heberle et al. [19] studied the second law efficiencies of zeotropic mixtures as the working fluids for a geothermal ORC. The results showed that the efficiency was increased up to 15% compared to that of pure fluid for heat source temperature below 120°C.

Deethayat et al. [20] studied a basic ORC using R245fa/R152a as the working fluids and the irreversibility at the evaporator and the condenser were found to be less than those of the unit using single R245fa. Anyhow, there was a limit of R152a composition due to its high flammability when the value was over 30%. In this study, performance analysis of a 50KW ORC

with internal heat exchanger was studied when the working fluid was a mixture of R245fa/R152a. A hot water stream at 115°C was taken as a heat source at the evaporator and a cool water stream fixed at 27°C was conducted as a heat sink at the condenser. The effects of evaporating temperature, mass fraction of R245fa and effectiveness of internal heat exchanger on the ORC performances following the first law and the second law of thermodynamics were considered.

Fiaschi et al. [21] investigated possibility of using an absorption heat transformer to enhance low-enthalpy geothermal water temperature for producing electricity throughout ORC power plant.

Gozdur and Nowak [22] found that the cycle efficiency is not a sufficient criterion for assessment of the ORC. Regarding the ORC–CHP systems energized by geothermal water, few activities and researches have been conducted for different assumptions and evaluations.

Li et al. [23] analyzed the series and parallel circuit geothermal systems (100–150℃) in oil field using ORC under consideration of various working fluids. The results showed that R601a has the highest cycle performance within the scope of that study and the series circuit with a pre heater has higher efficiencies than that without.

Tempesti et al. [24] presented a thermoeconomic analysis of a micro-Combined Heat and Power (CHP) plant operating through an ORC using the geothermal (80–100℃) and solar energies. The results showed that R245fa allows the lowest price of electricity production and the lowest overall cost of the CHP plant.

Khennich et al. [25] modeled two CHP systems with ORC and R134 a as working fluid. The both systems generated less mechanical power than the heat delivered to the heating load and a higher fraction of the heat source was used as the heating load increases.

Mago et al. [26] analysed the exergy destruction in Organic Rankine Cycle. Visual representations using an exergy wheel clearly show the exergy accounting for each

thermodynamic process. The results show that the evaporator has by far the highest exergy destruction rate, followed by the turbine. Therefore, it seems that cycle modifications, of which the aim is to reduce exergy destruction in the evaporator, have a major potential to increase the power output of the ORC.

Roy et al. [27] studied the output power, the second and first law efficiency and irreversibilities of an ORC using R12, R123 and R134a as working fluids. The ORC was driven by flue gas waste heat at 140℃. Their results show that the point of maximum thermal efficiency and maximum power output do not coincide. Furthermore the second law efficiency is strongly affected by the pinch point temperature difference in the evaporator.

Heberle et al. [28] investigated the second law efficiency of an ORC with zeotropic mixtures of isobutene/isopentane and R227ea/R245fa as working fluids. The results show that for temperatures below 120℃ the second law efficiencies increased in the range of 4.3–15%. The optimal second law efficiency was achieved when the temperature glide of condensation and cooling water matched.

Ho et al. [29] compared the Organic Flash Cycle (OFC) to an optimized basic ORC cycle, a zeotropic Rankine cycle with a binary ammonia–water mixture and a transcritical CO_2 cycle. A distinction is made between utilization efficiency and second law internal efficiency. The former definition assumes that the exergy which is left in the waste heat stream is discarded or unused, while the latter discards exergy destruction due to heat transfer in the evaporator. The definition of second law efficiency is therefore not unique; it is based on a carefully selected set of chosen input and output streams.

Liu et al. [30] analyzed the influence of the temperature glide during the zeotropic condensing process on the thermal efficiency, exergy efficiency and output work of ORC system. Based on the experimental result of the exhaust gas under varying operating conditions.

Yang et al. [31] studied the system performance of eight zeotropic mixtures as working fluids in a waste heat recovery system of vehicle engine.

Wang and Zhao [32] compared three different compositions (0.9/0.1, 0.65/0.35 and 0.45/0.55) of R245fa/R152a to pure R245fa at a low temperature solar ORC. In order to investigate the second law efficiency of subcritical cycles.

Garg et al. [33,34] respectively used isopentane/R-245fa, CO_2/isopentane and CO_2/propane as working fluids, and evaluated the system performance. A technique of identifying the required source temperature for a given output of the plant and the maximum operating temperature of the working fluid is developed by the authors. For the heat source temperature of 150℃ and 250℃, when using mixtures as the working fluids of ORC systems.

Chys et al. [35] found a potential increment of 16% and 6% in system efficiency respectively. The power generation at optimal condition can be increased by 20% for the low temperature heat source comparing with the pure working fluids.

Venkatarathnam et al. [36] considered that there were certain limits for the temperature glide of the heat transfer fluid in the evaporator and condenser to avoid pinch point, which could be used to evaluate the suitability of zeotropic mixtures for glide matching.

Chen et al. [37] proposed a supercritical Rankine cycle using zeotropic mixtures for the low grade heat. The result showed that thermal efficiencies of the cycles using mixtures (0.7R134a/0.3R32) were 10–30% higher than the cycle with pure R134a.

Saleh et al. [38] examined 31 pure fluids with ORC cycle operating temperature of less than 100℃. The results show that the thermal efficiency ranges between 3.6% and 13% depending on choice of working fluid and rises with increasing critical pressure of the fluid.

Tchanche et al. [39] evaluated 20 working fluids for a solar ORC micro-power system. For the chosen boundary conditions R134a, R152a and R600 are the most suitable fluids.

Papadopoulos et al. [40] proposed a holistic approach for fluid selection. By the use of computer aided molecular design in conjunction with process optimization physical, chemical, environmental, safety and economic properties of pure ORC fluids were evaluated.

Bliem [41] investigated the use of R114/R22 for geothermal power generation. The mixture shows between 3% and 8% higher efficiency compared to R114. It should be noted that these fluids are forbidden by law nowadays.

Gawlik and Hassani [42] demonstrated that levelized equipment costs can be reduced by using mixtures instead of pure fluids in geothermal binary plants.

Borsukiewicz [43] analyzed different pure fluids and a propane/ethane mixture for low-temperature ORC. They observed a higher power output at similar thermal efficiency for the equimolar propane/ethane mixture compared to pure propane.

Lakew et al. [44] stated that when a heat source with temperature ranging from 80 to 160℃, using R227ea resulted in a maximum power output; when heat source temperature ranged from 160 to 200℃, using R245fa could obtain a maximum power.

2.2 WORKING FLUID SELECTION

Efficient operation of an Organic Rankine Cycle is primarily a function of two parameters: the working conditions of the cycle and the thermodynamic properties of the working fluid used in the cycle. Three main types of working fluids exist that can be used in ORC. These types are classified by their slope on the vapour side of the saturation curve. The plot in fig.2.1 is a simple saturation dome that has been cut off after the inflection point in order to display the different type of fluid slopes. Fig.2.1 below shows a comparison of the types of fluids classified by their slopes on a T-s diagram. Note that this diagram does not directly reflect any specific fluids it is simply a graphic display of the possible types of fluids and their slopes [45,46].

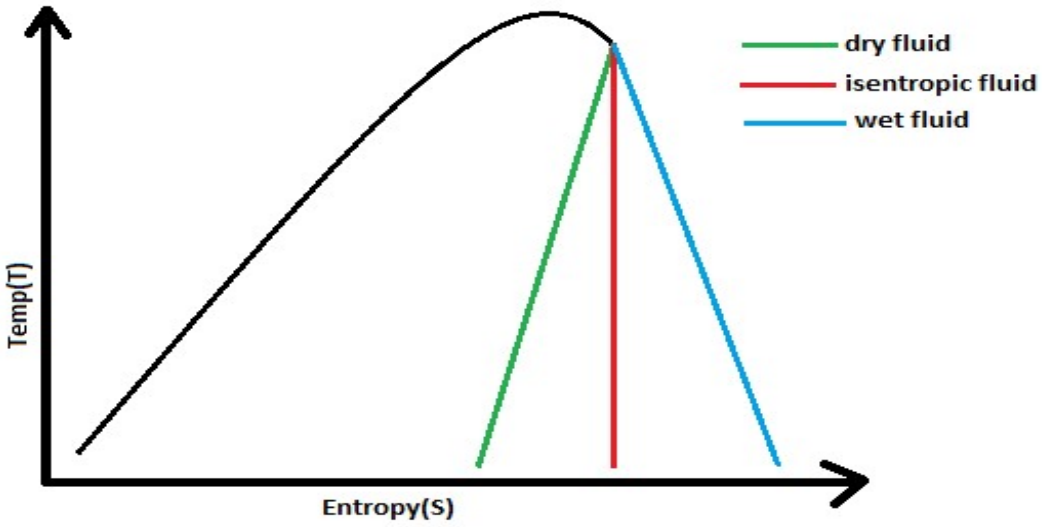

Fig.2.1 T-S diagram for different fluid types

A fluid that has a negative slope, such as the blue line in fig.2.1, is called a wet fluid. The most common wet fluid is water but other wet fluids include: ethanol, methane, hydrogen, DME and most fuels. A fluid that has a positive slope, such as the green line in fig.2.1, is called a dry fluid. Common dry fluids include: toluene, n-pentane, isopentane, R-245fa, Isobutane and many refrigerants. A fluid that has an infinite slope, such the red line in fig.2.1, is called an isentropic fluid. Common isentropic fluids include: benzene, R-11, R-123, and hexane. The different types of fluids can vary the thermal efficiency of the ORC and each type can offer a different advantage when it is used within the cycle.

For instance, isentropic fluids are best at recovering low temperature waste heat whereas wet fluids are best at recovering high temperature waste heat and dry fluids are able to be used with a recuperator. The different types of fluids mainly affect the state of the working fluid at the exit of the turbine. Since the vapour-saturation curve for a wet fluid has a negative slope it is possible to be in a two-phase region after undergoing isentropic expansion in the turbine, if it is not highly superheated in the evaporator. This can be seen by drawing a vertical line starting at the pressure and temperature specified and ending at the final temperature and entropy. If this line lies in the saturation dome then it is possible that the fluid is still in the two-phase region. Since an

isentropic fluid has an infinite slope on the vapour saturation curve the saturated vapour at the inlet to the turbine remains saturated throughout an isentropic expansion in an ideal turbine. Since a dry fluid has a positive slope on the saturation vapour curve when it undergoes an isentropic expansion in the turbine the fluid is superheated at the exit of the turbine.

A wet fluid, as seen in fig.2.1, is the most unlikely choice for an ORC since it is most efficient utilizing high temperature waste heat. Wet fluids have a critical point which occurs at a far greater temperature then that of dry and isentropic fluids which makes them more efficient at higher pressures and higher temperatures. Since wet fluids have high molecular numbers they are more complex and have a higher ability to store heat than the less complex and lower molecular numbered dry fluids. A wet fluid is usually used to transfer heat from the waste heat source and from the cooling source to the ORC since it has a high heat capacity. This can be seen through the following equation.

The specific heat of a fluid can be written as follows in order to relate temperature, entropy, and specific heat.

$$C_P = C_V + R = T \times \left(\frac{\partial S}{\partial T}\right)_V + R \tag{2.1}$$

In the equation above; C_p is the specific heat of the fluid at constant pressure, C_v is the specific heat of the fluid at constant volume, T is the temperature of the fluid at a given state, and $\left(\frac{\partial S}{\partial T}\right)_V$ is the partial derivative of entropy with respect to temperature at a constant volume. By comparing the slopes on the vapour side of the saturation dome for wet and dry fluids one can see that the slope for a dry fluid is a much steeper than the slope for a wet fluid. In a T-s diagram the slope is the change in temperature divided by the change in entropy. This relation is the inverse of the term in equation 2.1. Since the inverse of a large number is very small, a fluid with a steep slope would have a lower C_p than a fluid with a gradual slope. This shows that wet fluids have a higher heat capacity than dry fluids and should be used in higher temperature situations or applications that require a lot of heat to be delivered to a source [47].

The main advantage of using a dry fluid is that a recuperator heat exchanger can be used in the cycle to take the energy left in the superheated vapour at the exit of the turbine and use it to preheat the fluid entering the evaporator. The use of a recuperator increases the overall thermal efficiency of the cycle and reduces the amount of heat input and output to and from the cycle. Turbines are easily damaged by moisture contained in the vapour that is expanded in the turbine. Dry fluids cause less damage on turbines, compared to wet fluids, since they are superheated throughout the expansion within the turbine. This is a great advantage to dry fluids since the wear and tear on the turbine is less which yields and overall longer life of the turbine.

An isentropic fluid is very efficient at recovering low temperature waste heat and may be the best choice of working fluid depending on whether a recuperator is desired. Isentropic fluids have a lower critical temperature than wet fluids which makes them more efficient at recovering low temperature waste heat than wet fluids. The overall area within the saturation dome is greater for an isentropic fluid than a dry fluid. This means that the maximum work achievable by a cycle using an isentropic fluid is greater than that of a dry fluid. The choice of the working fluid greatly affects the thermal efficiency of the ORC. According to a study done by T.C. Hung et al [17], the efficiency of the cycle is closely related to the latent heat of the fluid at low pressure; a greater latent heat at low pressure yields a lower efficiency since a larger portion of the energy carried by the fluid is rejected via the condenser. The efficiency is also a weak function of the turbine inlet temperature, i.e. an increase of superheat in the turbine does not result in a significant increase in efficiency.

The efficiency of the ORC increases nearly linearly with the turbine-inlet temperature. Unlike wet fluids, dry fluids show decreased efficiency as the turbine-inlet temperature is increased, except when the system pressure is very high. This result indicates that the optimum efficiency occurs if dry fluids operated along the saturation curve without being superheated.

Isentropic fluids exhibit trends similar to wet fluids except that the increase of efficiency levels off as the temperature is increased. The system efficiency also increases as the system pressure increases. The working fluid yields more work during the isentropic expansion process if the turbine-inlet pressure is raised. However, raising the system pressure is not always feasible for

economic reasons since the capital costs for the waste-heat boiler and piping system, as well as system complexity and material selection of the components, must also be considered. Therefore the choice of the working fluid depends greatly on the desired outcome of the ORC, i.e. if a recuperator is desired, if higher output is desired, or if higher thermal efficiency is desired.

The choice of the optimal working fluid depends basically on the heat source and the heat sink temperature. For any heat temperature level there are a number of candidates which show a good match between heat source and heat sink temperatures and cycles boundary conditions. The choice the right working fluid is not an easy process. The fluid selection process is a trade-off between thermodynamic specifications, safety, environmental and economy aspects. The following criteria should be taken in consideration in order to figure out the best candidates.

2.2.1 THERMODYNAMIC PROPERTIES

Thermodynamic properties are of key importance in the design process of organic Rankine cycle, regarding optimal energy utilization and reducing exergy losses. The following are some important thermodynamic properties for working fluids [47]:

- For a certain heat sink and heat source the Net Power Out, the thermal efficiency and the second law efficiency should be as high as possible.
- The condensing pressure should be higher than the atmospheric pressure to avoid leakage issues.
- In sub-critical cycles the critical pressure for the working fluid must be higher than the pressure in the evaporator.
- Vapor density

The higher the density, the lower the specific volume and volumetric flow rate. Low volumetric flow is desirable to achieve smaller component and more compact machines. Low density fluids have high specific volume and need bigger components (heat exchangers and expander). A bigger component size leads to more expensive units and more costly systems. Furthermore, a high specific volume increases the pressure drop in the heat exchangers and needs higher pump work.

- Large enthalpy variation in the turbine leads to high net work output.

- Higher convective heat coefficient and high-thermal conductivity increases the heat transfer process between the heat source, the heat sink and the working fluid.
- High heat capacity (C_p) of the liquid leads to better energy recovery from the heat source and decrease the mass flow rate of the working fluid.
- The working fluid should be thermally and chemically stable.

2.2.2 HEAT TRANSFER PROPERTIES

Heat transfer properties are of key importance and a very important parameter in sizing heat exchangers. High C_P value makes working fluid absorbs efficiently the thermal energy from heat source. High C_P allows a better temperature profile approaches in the heat exchangers and improves efficiencies. There are many factors affecting the heat transfer process. Some factors are related to the cycle architecture including piping design, flow rates (Reynolds number) and material selection. Other factors are related to the working fluid properties and affect the overall heat transfer capability. The working fluid thermal conductivity (k), specific heat (C_P) and viscosity (μ) are three key properties used to calculate Prandtl numbers ($Pr = \mu * C_P/k$) which are widely used in heat exchanger design. It is desirable to have a working fluid with a viscosity as low as possible, and a specific heat and thermal conductivity as high as possible [47].

2.2.3 ENVIRONMENTAL AND SAFETY CRITERIA

Environmental and safety criteria are of key importance in working fluid selection however many working are phased out or on the way to be. The phased out working fluids have high ozone depletion potential ODP and global warming potential GWP. Some working fluids have good thermodynamic properties but at the same time have undesirable environmental and safety effects [48].

According to EC Regulation 2037/2000, many working fluids like CFC, CFCs and HCFCs refrigerant are already phased out. These refrigerants are banned due to their ozone depletion potential ODP and global warming potential GWP.

The EC Regulation 2037/2000 affects users, producers, suppliers, maintenance and servicing engineers, and those involved in the disposal of all ozone depletion substances ODS. The new

regulation includes chlorofluorocarbons (CFCs), hydrochlorofluorocarbons (HCFCs), halons, 1,1,1 trichloroethane, carbon tetrachloride and bromochloromethane (CBM). These refrigerants are mainly used in refrigeration, air-conditioning, foam blowing, as solvents and in fire fighting.

2.2.3.1 Environmental data

The environmental data includes global warming potential GWP and ozone depletion potential ODP.

(a) Global Warming Potential (GWP)

The number of Global Warming Potential (GWP) refers to the amount of global warming caused by a certain working fluid relative to CO_2 for a 100 year time-frame. Or in other words, the GWP is the ratio of the warming caused by a substance to the warming caused by a similar mass of carbon dioxide. Thus, the GWP of CO_2 is defined to be 1.0. Water has a GWP of 0. Carbon dioxide is used as reference because it has the greatest net impact on global warming. There are some other refrigerants which typically have a higher GWP than carbon dioxide but they are available in much smaller quantities

(b)Ozone Depletion Potential (ODP)

The Ozone Depletion Potential (ODP) refers to refrigerants' and other chemicals' ability to destroy stratospheric ozone relative to R11. According to the United States Environmental Protection Agency EPA the Ozone Depletion Potential ODP is: "The ratio of the impact on ozone of a chemical compared to the impact of a similar mass of CFC-11. Thus, the ODP of CFC-11 is defined to be 1.0. Other CFCs and HCFCs have ODPs that range from 0.01 to 1.0. The halons have ODPs ranging up to 10. Carbon tetrachloride has an ODP of 1.2, and methyl chloroform's ODP is 0.11. HFCs have zero ODP because they do not contain chlorine".

2.2.3.2 Safety data

The safety data in this thesis includes the lower flammability level LFL and safety classification of working fluids and refrigerants.

(a) Lower flammability limit (LFL)

The lower flammability limit LFL is usually measured in volume percent and refers to the lower end concentration of a flammable solvent in ambient air when the mixture can ignite in a given temperature and pressure. There is a variation in LFL values among separate laboratories and that is because they use different vessels or ignition sources or different evaluation standards.

(b) Safety classification

According to ASHRAE standard 34 (ASHRAE, 2010a and 2010b) the letters A refers to "lower" toxicity while the letter B means higher toxicity. The numbers 1,2 and 3 refer to flame propagation, number 1 means no flame propagation, number 2 means lower flammability and number 3 means higher flammability. The shortening "wwf" indicates the worse case of fraction of flammability or worse case of formulation, and it means that the working fluid is flammable in either vapor or liquid phase. In some cases group 2 is signified with letter L (like A2L and B2L) and here the letter L means more difficult to ignite.

Table1. Safety classification [48]

	Lower toxicity	**Higher toxicity**
Higher flammability	A3	B3
Lower flammability	A2	B2
No flame propagation	A1	B1

2.3 RESEARCH GAP

On the basis of literature survey, many research works have been done on the performance analysis of geothermal organic Rankine cycle using zeotropic mixtures. Apart from this, performance analysis of geothermal organic Rankine cycle using zeotropic mixture of R600a/DME has not been done and performance of regenerative and superheated cycle using this mixture has not been done also.

2.4 OBJECTIVE OF PRESENT WORK

In this work, First law (energy) and Second law (exergy) analysis of geothermal organic Rankine cycle has been carried out using a zeotropic mixture of R600a/DME.

The objectives are:

1. To calculate the net work output, thermal efficiency and exergetic efficiency of geothermal organic Rankine cycle using zeotropic mixture of R600a/DME in six different proportions for various evaporator inlet temperatures.
2. To compare the net work output, thermal efficiency and exergetic efficiency in order to evaluate performance of ORC for various inlet evaporator temperatures.
3. To evaluate and compare the irreversibility in each component of system for each proportion of mixture by varying evaporator inlet temperature.
4. To calculate mass flow rate of zeotropic mixture for various inlet temperatures to evaporator.

CHAPTER -3
THERMODYNAMIC ANALYSIS

3.1 SYSTEM DESCRIPTION

The working principles for the ideal organic Rankine cycle are similar to the ideal Rankine cycle. The condensate working fluid is pumped from the condenser where the pressure is low to the evaporator where the pressure is high. The process takes place at constant entropy. The high pressure liquid enters the evaporator and absorbs the thermal energy from heat source at constant pressure. In this process the refrigerant changes the phase from saturated liquid to saturated or superheated vapor. The external heat source can be waste heat from industry, geothermal heat, solar heat, biomass etc. The high pressure saturated or superheated vapor leaves the evaporator and expands through an expander at constant entropy to produce mechanical work. Under the expansion process, the pressure decreases to condenser pressure. After expansion process the working fluid leaves the expander and enters the condenser as unsaturated, saturated or superheated vapor depending on working conditions and the type of used working fluid. In the condenser, the working fluid condensates and changes phase to saturated or undercooled liquid with the help of a heat sink, and then the cycle is repeated.

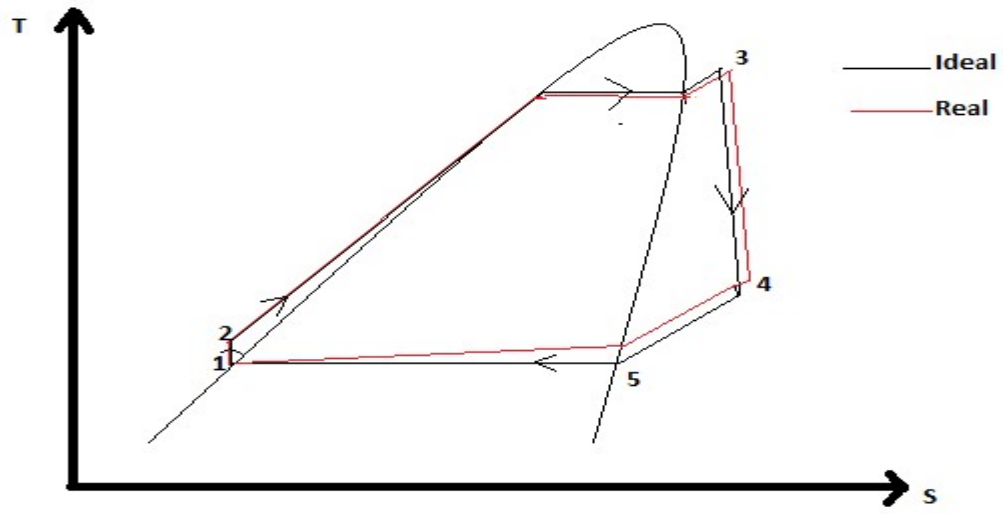

Fig.3.1 Ideal and real Organic Rankine Cycle

In the real cycle the compression and expansion processes are not isentropic and there are always some losses in the pump and the expander. The heat addition and heat rejection processes are not isobaric and there are always pressure losses in the piping system. The irreversibility affects very much the performance of the thermodynamic system.

In a real cycle, there are two main sources for entropy generation and these sources are external and internal. The internal entropy generation occurs due to

- Pressure drop because of friction in the system associated pipes
- Un-isentropic compression and expansion in the compressor or expander
- Internal transfer of energy over a finite temperature difference in the components.

And the external entropy generation occurs due to

- The mechanical losses during work transfer
- Heat transfer over the finite temperature difference

Organic Rankine cycle has the same working principles and main components (evaporator, condenser, expander and pump) as the steam Rankine cycle. The main difference between the two cycles is the working fluid utilized. Fig.3.2 shows the T-S diagram for a basic organic Rankine cycle and fig.3.3 shows the cycle layout.

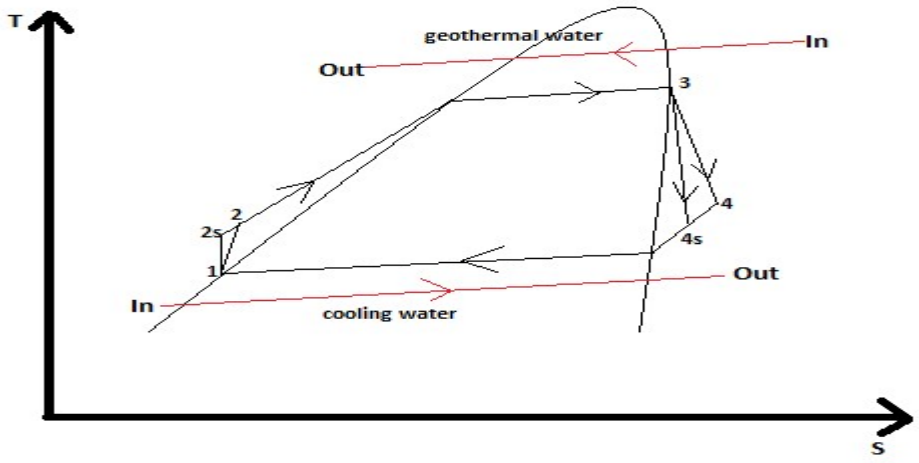

Fig.3.2 T-S diagram of actual organic Rankine cycle

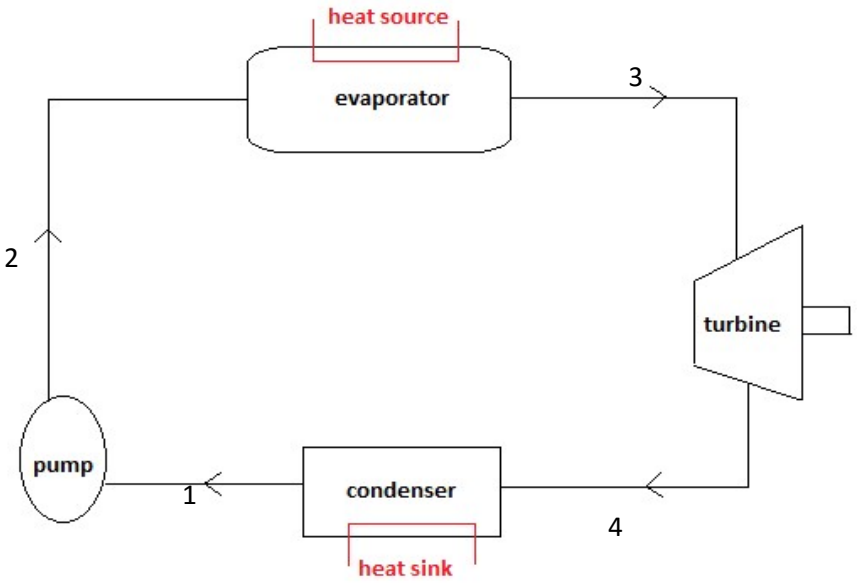

Fig.3.3 Basic layout of organic Rankine cycle

3.2 ENERGY ANALYSIS

The following assumption have been made in analysis of organic Rankine cycle

- Kinetic energy and potential energy of operating process were neglected.
- No pressure drop and heat loss were considered in the pipes.
- Temperature difference at the pinch point is set to be 10K.

Process (1 – 2) Compression

The working fluid leaves the condenser as saturated liquid and then it is pumped to the evaporator pressure at constant entropy. The state of the working fluid at pump inlet is indicated by point 1 and at pump outlet by point 2 (fig.3.2). The power absorbed by the pump is estimated by equation (3.1)

$$W_{pump} = \dot{m}_1 \times (h_2 - h_1) \quad (3.1)$$

$$\eta_p = (h_{2s} - h_1)/(h_2 - h_1) \quad (3.2)$$

Where

W_{pump} is the work consumption by pump (kW)

$\dot{m}_1$ is the mass flow rate of organic fluid (kg/s)

h_1 is specific enthalpy at pump inlet (kJ/kg)

h_2 is actual specific enthalpy at pump outlet (kJ/kg)

h_{2s} is isentropic specific enthalpy at pump outlet (kJ/kg)

η_p is isentropic efficiency of pump

Process (2-3) Heat addition

In this process heat is added to the working fluid at constant pressure, the process can be considered isobaric. The working fluid's state out of the evaporator is indicated by point 3 and the heat added to the working fluid can be calculated by equation (3.3).

$$Q_{evp} = \dot{m}_1 \times (h_3 - h_{2)} \tag{3.3}$$

Where

Q_{evp} is heat added to the working fluid in evaporator (kW)

h_3 is the actual vapor enthalpy out of the evaporator and into the expander (kJ/kg)

Based on first law of thermodynamics, the following energy balance equation is used between evaporator and heat source.

$$\dot{m}_1 \times (h_3 - h_2) = \dot{m}_2 \times c_{pw} (T_{in} - T_{pp}) \tag{3.4}$$

$\dot{m}_2$ is mass flow rate of geothermal water (kg/s)

c_{pw} constant pressure specific heat of geothermal water (kJ/kgK)

T_{in} inlet temperature of geothermal heat source (K)

T_{pp} pinch point temperature in evaporator (K)

Process (3-4) Expansion

This is an expansion process and the absorbed energy at the evaporator is converted to useful mechanical work by an expander or a turbine. The state of the working fluid out of the expander is indicated by point 4 and the useful work out can be estimated by equation (3.5).

$$W_{turb} = \dot{m}_1 \times (h_3 - h_4) \quad (3.5)$$

$$\eta_t = (h_3 - h_{4s})/(h_3 - h_4) \quad (3.6)$$

W_{turb} is the work produced by the turbine (kW)

h_4 is the actual specific enthalpy at turbine outlet (kJ/kg)

h_{4s} is isentropic specific enthalpy at turbine outlet (kJ/kg)

η_t isentropic efficiency of turbine

Process (4-1) Heat rejection

In this process the heat is rejected in condenser in order to condensate the working fluid and re-circulates it in the cycle. The heat rejection process is considered to be isobaric. The working fluid leaves the condenser as saturated. Point 1 refers to the working fluid at condenser outlet and pump inlet in T-S diagram. The amount of heat rejected can be estimated by equation (3.7).

$$Q_{con} = \dot{m}_1 \times (h_4 - h_1) \quad (3.7)$$

Where

Q_{4-1} stands for the heat rejected heat in condenser (kW)

Thermal efficiency is defined as ratio of the net work output to heat supplied to the evaporator.

$$\eta_{th} = (W_{3-4} - W_{1-2})/Q_{2-3} \quad (3.8)$$

3.3 EXERGY ANALYSIS

Exergy destruction in pump

The exergy destruction rate in the pump is given by equation (3.9)

$$\dot{I}_{pump} = \dot{m}_1 \times T_0(s_2 - s_1) \quad (3.9)$$

Where

$\dot{I}_{pump}$ is the exergy destruction rate in the pump (kW)

T_0 is ambient temperature (K)

s_1 is specific entropy at pump inlet (kJ/kgK)

s_2 is specific entropy at pump outlet kJ/kgK)

Exergy destruction in evaporator

The temperature of the heat source decreases through the evaporator. Taking the arithmetic mean temperature (T_H) between inlet and outlet temperature, $T_H = (T_{in} + T_{pp})/2$, the energy destruction in evaporator can be estimated by equation (3.10).

$$\dot{I}_{evp} = \dot{m}_1 \times T_0[(s_3 - s_2) - (h_3 - h_2/T_H)] \quad (3.10)$$

Where

$\dot{I}_{evp}$ is the exergy destruction rate in the evaporator (kW)

s_3 is specific entropy at evaporator outlet kJ/kgK)

Exergy destruction in turbine

Equation (3.11) gives the exergy destruction rate in the expander.

$$\dot{I}_{turb} = \dot{m}_1 \times T_0(s_4 - s_3) \quad (3.11)$$

$\dot{I}_{turb}$ is the exergy destruction rate in turbine (kW)

s_4 is specific entropy at turbine outlet (kJ/kgK)

Exergy destruction in condenser

Since heat sink temperature increases continuously from condenser inlet to condenser outlet, the arithmetic mean temperature, $T_L = (T_{ci} + T_{co})/2$ can be used to estimate the exergy destruction in the condenser. Equation (3.12) gives the exergy destruction in the condenser.

$$\dot{I}_{con} = \dot{m}_1 \times T_0[(s_1-s_4)-(h_1-h_4/T_L)] \quad (3.12)$$

$\dot{I}_{con}$ refers to the exergy destruction rate in condenser (kW)

The system's total energy destruction can be calculated by combining equations 3.9, 3.10, 3.11 and 3.12.

$$\dot{I}_{total} = \dot{I}_{1-2} + \dot{I}_{2-3} + \dot{I}_{3-4} + \dot{I}_{4-1}$$

Which gives

$$\dot{I}_{total} = \dot{m}_1 \times T_0 \times \left[\frac{h3-h2}{TH} - \frac{h1-h4}{TL}\right] \quad (3.13)$$

$$\textbf{Exergetic efficiency} = \frac{Wnet}{Wnet + \dot{I}total} \quad (3.14)$$

3.4 INPUT PARAMETER

The following input parameters have taken for the analysis of organic Rankine cycle:

- Ambient temperature (T_o) 298K
- Inlet temperature of geothermal heat source (T_{in})[49] 393K
- Mass flow rate of geothermal water (m_2)[50] 5 kg/s
- Inlet temperature of cold source (T_{ci}) 293K
- Outlet temperature of cold source (T_{co}) 303K
- Evaporating temperature (T_e)[50] 323K-373K
- Temperature difference at pinch point (ΔT_{pp}) 10K
- Condensing temperature (T_c) 308K
- Isentropic efficiency of pump (η_p) 75%
- Isentropic efficiency of turbine (η_t) 85%
- Const. pressure specific heat of geothermal water (C_{pw})[51] 4.31kJ/kgK

3.5 ORGANIC WORKING FLUIDS

For the analysis of organic Rankine cycle, we have selected the zeotropic mixture of Isobutane (R600a) and Dimethylether (DME) in different proportion.

Table2. Thermal physical properties of selected organic working fluids [45]

Name	NBP(℃)	T_c(℃)	P_c(kPa)	ODP	GWP (100 yr)	Safety Group	Expansion State
R600a	-11·7	134·70	36·3	0	20	A3	Dry
DME	-24·8	127·23	53·4	0	20	A3	Wet

NBP is normal boiling temperature of fluid

T_c is critical temperature of fluid

P_c is critical pressure of fluid

ODP is ozone depletion potential of fluid

GWP is global warming potential of fluid

Expansion state is the state after the expansion in turbine

By carried out the thermodynamics analysis of geothermal organic Rankine cycle using zeotropic mixture for the condition stated above, various state points have been obtained. Also by using REFPROP software, many thermal physical properties of zeotropic mixture at various state points have been obtained. The computer program for the analysis is developed in EES software has been given in Appendix.

CHAPTER -4
RESULTS AND DISCUSSION

The organic Rankine cycle (ORC) using geothermal water as heat source is analysed for temperature ranges of zeotropic mixture of organic fluids at the inlet to the evaporator by developing a computer program on Engineering Equation Solver (EES32) and REFPROP 9. The performance parameters selected for the analysis are thermal efficiency, exergetic efficiency, net work output, irreversibility present in each component of system, mass flow rate of organic fluid etc.

The performance of geothermal organic Rankine cycle using zeotropic mixture of R600a/DME is analysed on the basis of First law of thermodynamics (Energy analysis) and Second law of thermodynamics (Exergy analysis). By this analysis, several graphs are drawn by varying different parameters of ORC and after this comparison is made among them also.

The analysis provide a useful picture that clearly shows the best possible thermal efficiency, exergetic efficiency, net work output etc for ORC for various evaporator inlet temperature and for different fraction of mass of Isobutane (R600a) and Dimethylether (DME).

4.1 NET WORK OUTPUT

Fig.4.1 to fig.4.6 show a variation of net work output of system against temperature of zeotropic mixture at the inlet to the evaporator for six different proportions. Fig.4.7 shows comparison of net work output of system against evaporator inlet temperature of mixture of R600a/DME for six different proportions.

By using mixture in ratio of R600a/DME (0.8/0.2), the system gives 100.2kW net work output corresponding to 343K inlet temperature to the evaporator, which is maximum output among different proportions.

By doing analysis, found that for each different proportion of mixture, system gives the maximum net work output for temperature range of 343K-353K. After 353K net work output of system starts decreasing.

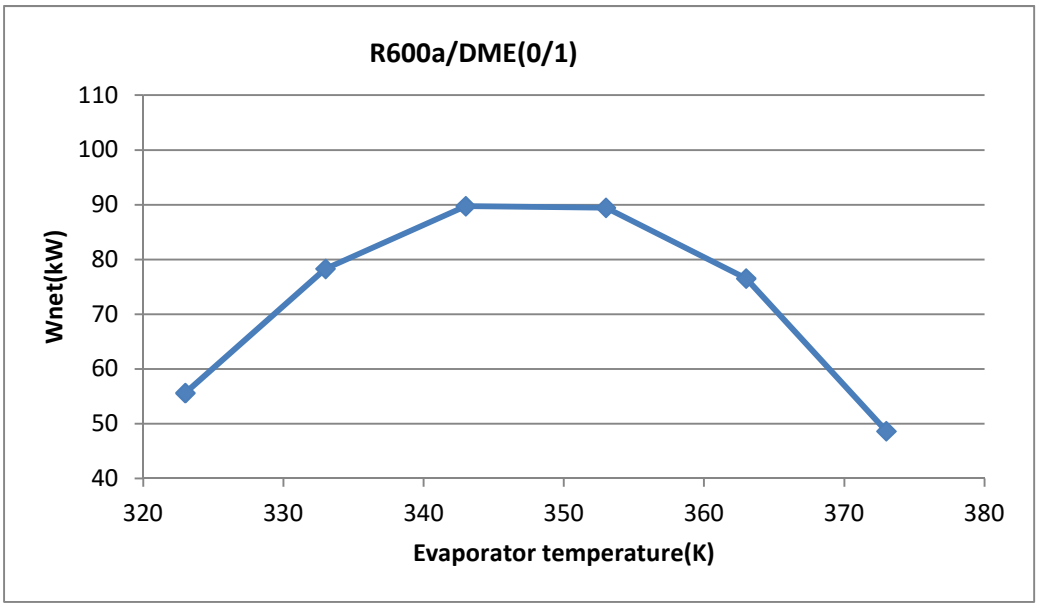

Fig.4.1 Net work output of system with temperature of mixture R600a/DME (0/1) at inlet to evaporator

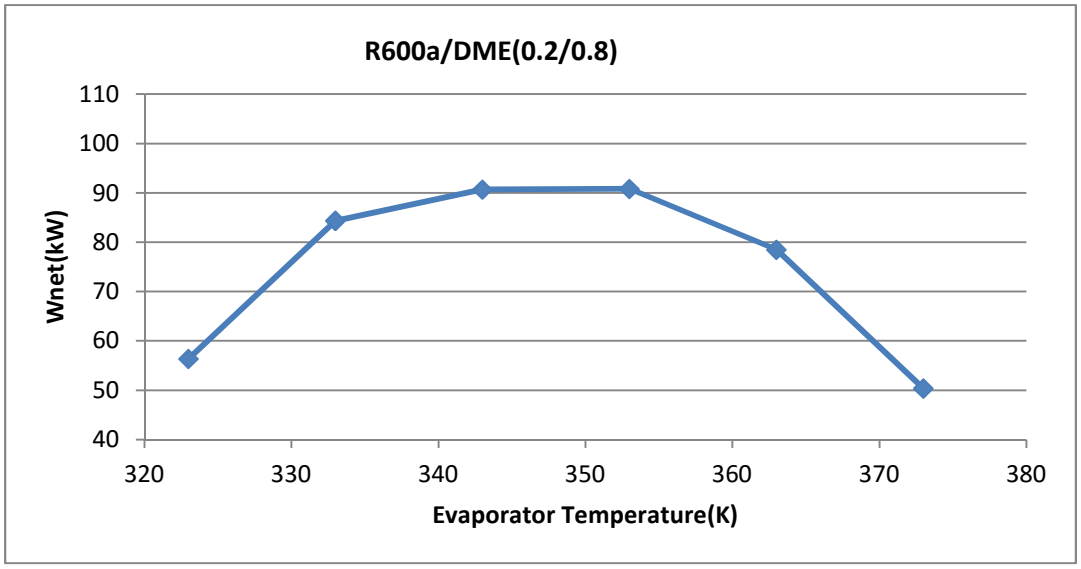

Fig.4.2 Net work output of system with temperature of mixture R600a/DME (0.2/0.8) at inlet to evaporator

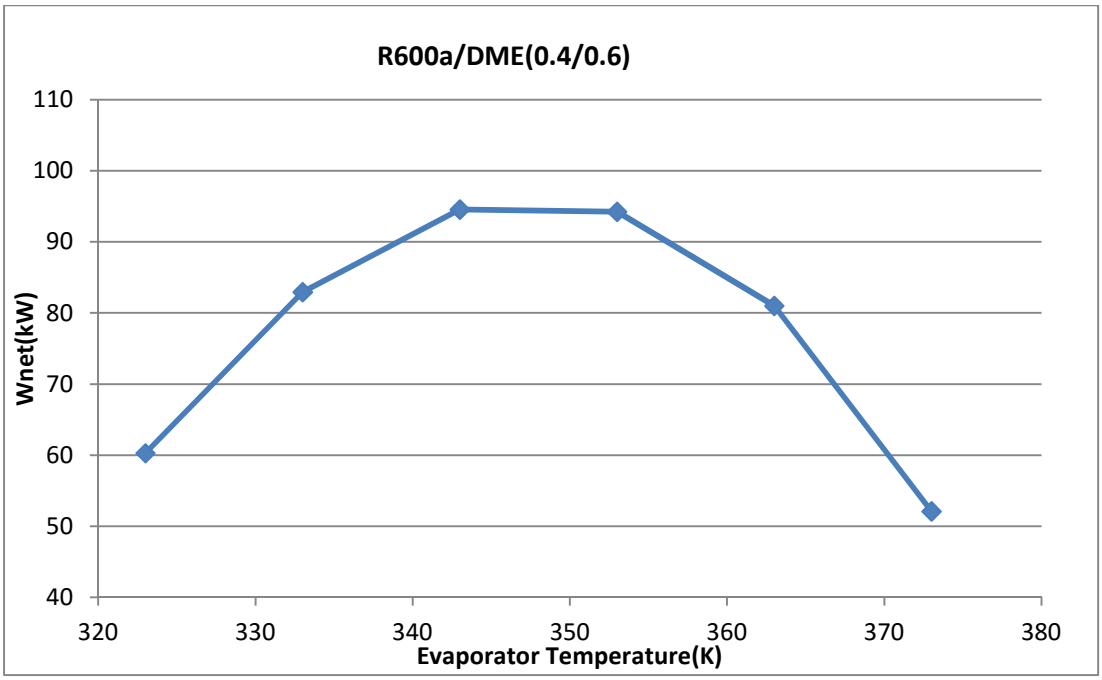

Fig.4.3 Net work output of system with temperature of mixture R600a/DME (0.4/0.6) at inlet to evaporator

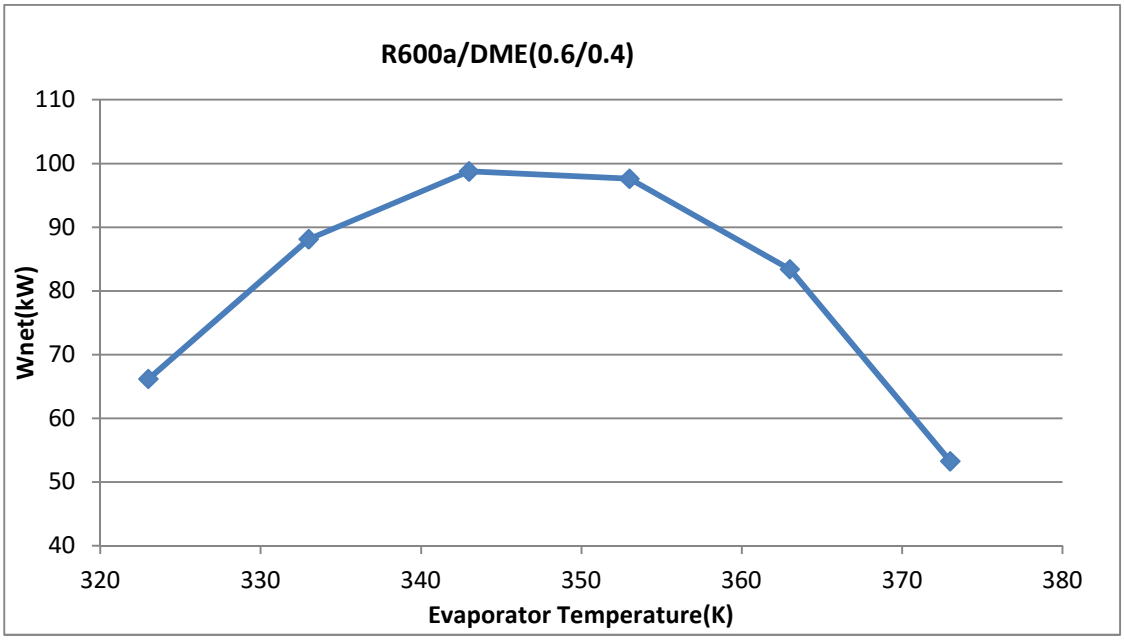

Fig.4.4 Net work output of system with temperature of mixture R600a/DME (0.6/0.4) at inlet to evaporator

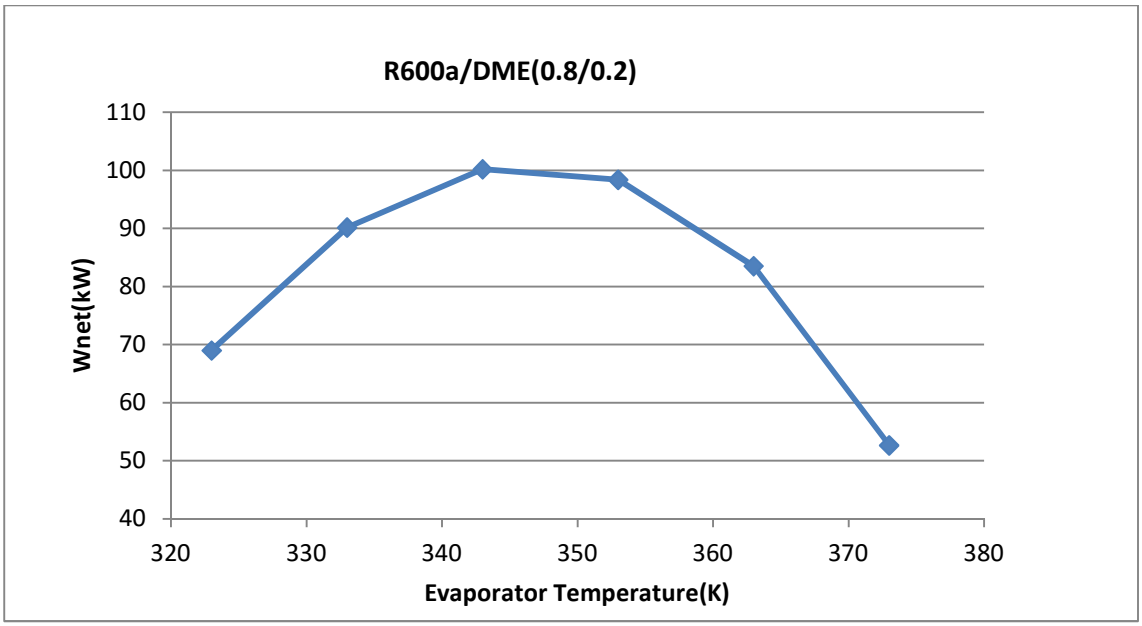

Fig.4.5 Net work output of system with temperature of mixture R600a/DME (0.8/0.2) at inlet to evaporator

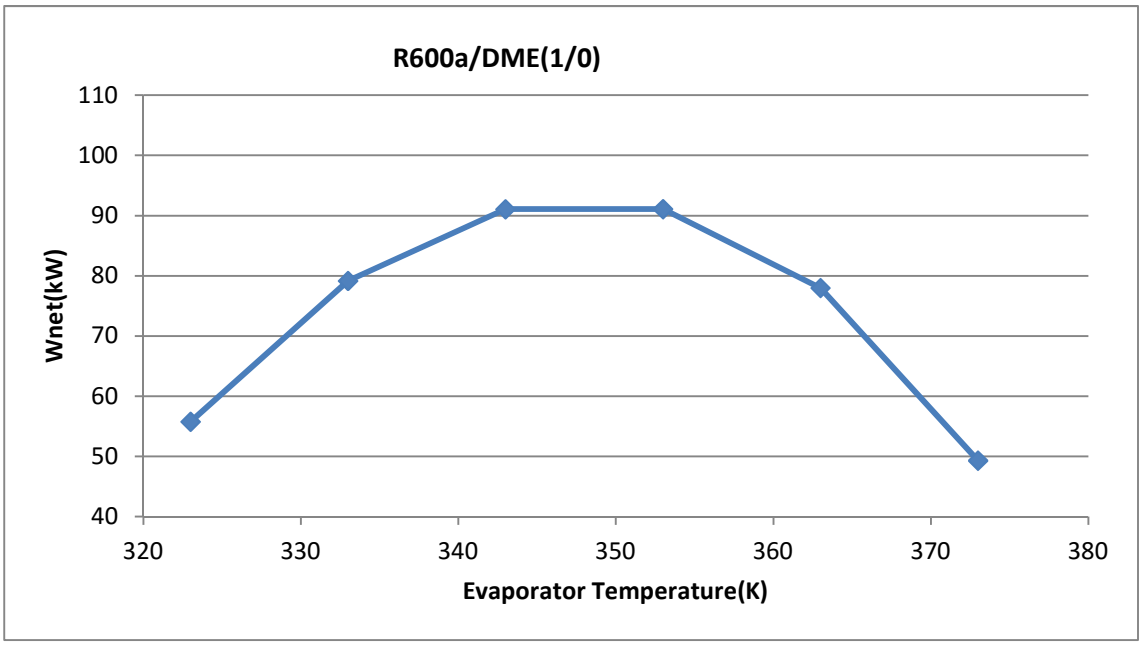

Fig.4.6 Net work output of system with temperature of mixture R600a/DME (1/0) at the inlet to the evaporator

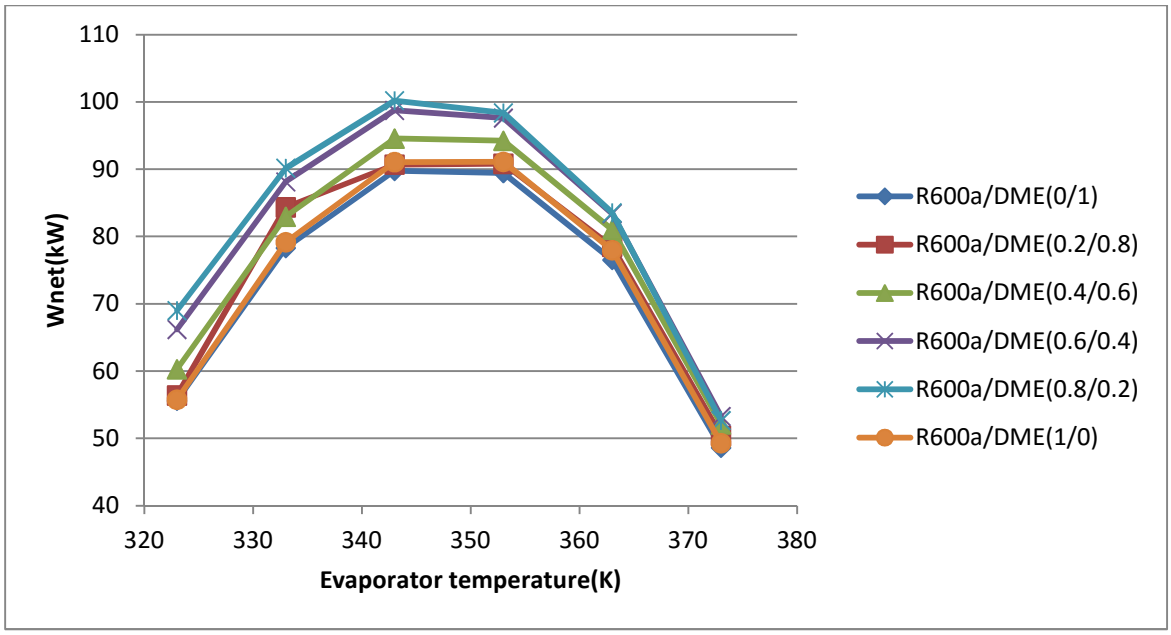

Fig.4.7 Comparison of variation of net work output of system against inlet temperature to evaporator of mixture for six different proportions

Table3. Comparison of net work output with different inlet temperature to evaporator for each proportion of mixture of R600a/DME

Inlet temperature To evaporator(K)	**Net work output (kW)**					
	Proportions of mixture of R600a/DME					
	0/1	**0.2/0.4**	**0.4/0.6**	**0.6/0.4**	**0.8/0.2**	**1/0**
323	55.61	56.37	60.28	66.19	69	55.76
333	78.3	84.35	82.95	88.13	90.17	79.16
343	89.75	90.69	94.56	98.75	100.2	91.07
353	89.45	90.81	94.24	97.61	98.39	91.1
363	76.52	78.49	81.01	83.41	83.53	77.98
373	48.63	50.37	52.09	53.27	52.67	49.3

4.2 THERMAL EFFICIENCY

Fig.4.8 to fig.4.13 show a variation of thermal efficiency against inlet temperature of zeotropic mixture to the evaporator for six proportions of mass of R600a/DME (0/1, 0.2/0.8, 0.4/0.6, 0.6/0.4, 0.8/0.2, 1/0) respectively. By increasing inlet temperature of zeotropic mixture to the evaporator, heat rejection reduces and output of turbine increases, due to which thermal efficiency of system continuously increases.

Fig.4.14 shows the comparison of thermal efficiency against evaporator temperature for all six proportions. Amongst all the selected proportions, R600a/DME (0.6/0.4) has the maximum thermal efficiency about 12.81% corresponding to 373K temperature of zeotropic mixture at the inlet to evaporator. R600a/DME (0/1) has second best thermal efficiency about 12.74% among these six proportions corresponding to 373K evaporator temperature. R600a/DME (1/0) has least 3.82% thermal efficiency corresponding to 323K temperature at inlet to the evaporator.

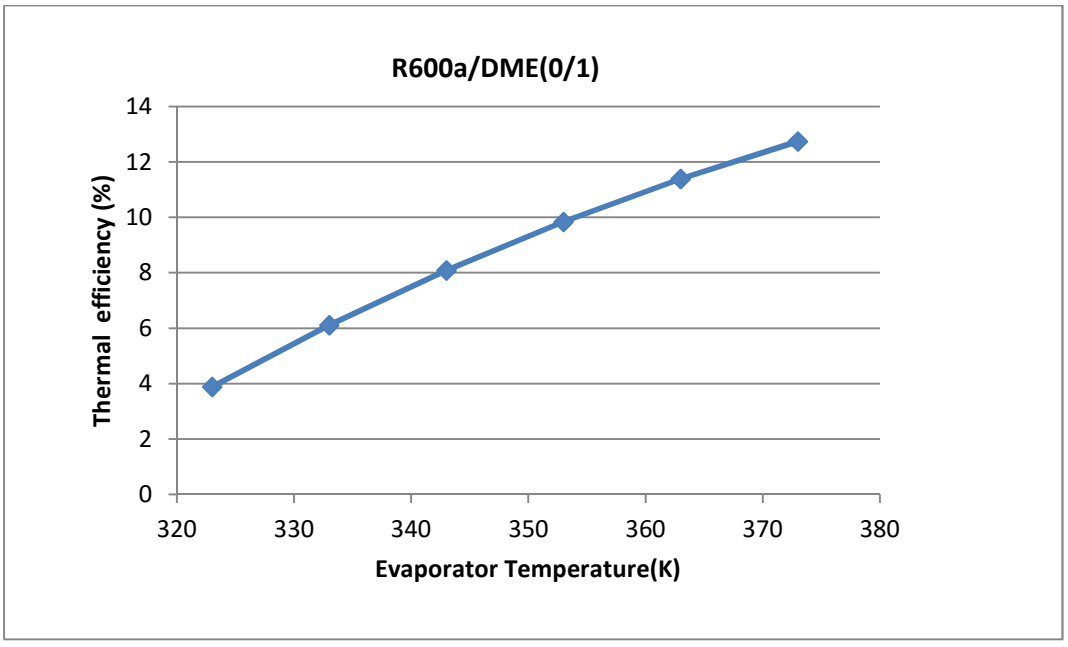

Fig.4.8 Variation of thermal efficiency with temperature of mixture R600a/DME (0/1) at inlet to evaporator

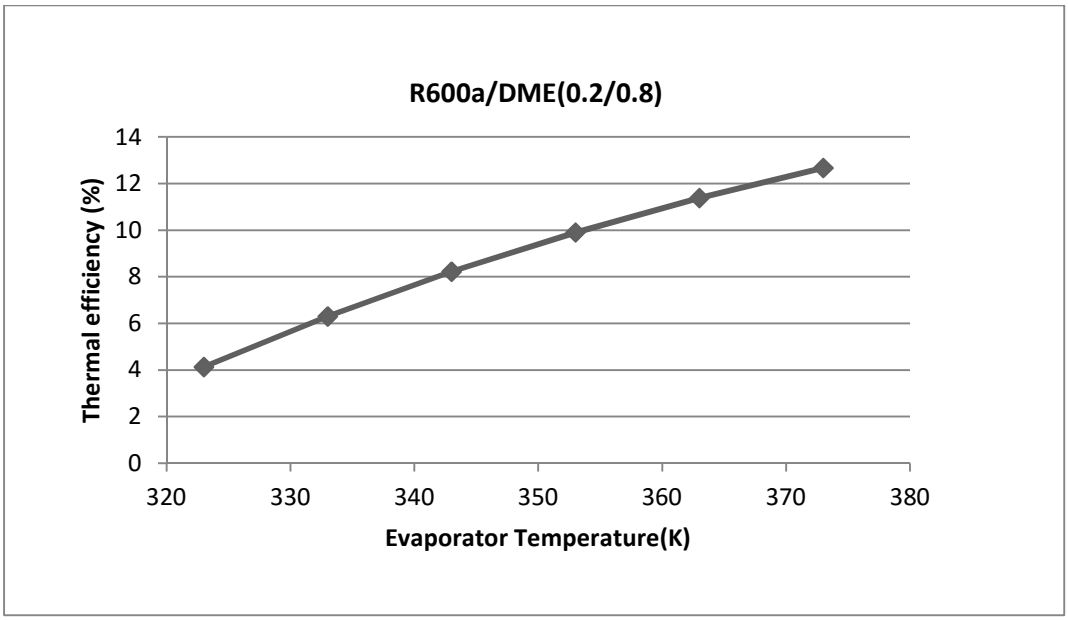

Fig.4.9 Variation of thermal efficiency with temperature of mixture R600a/DME (0.2/0.8) at inlet to evaporator

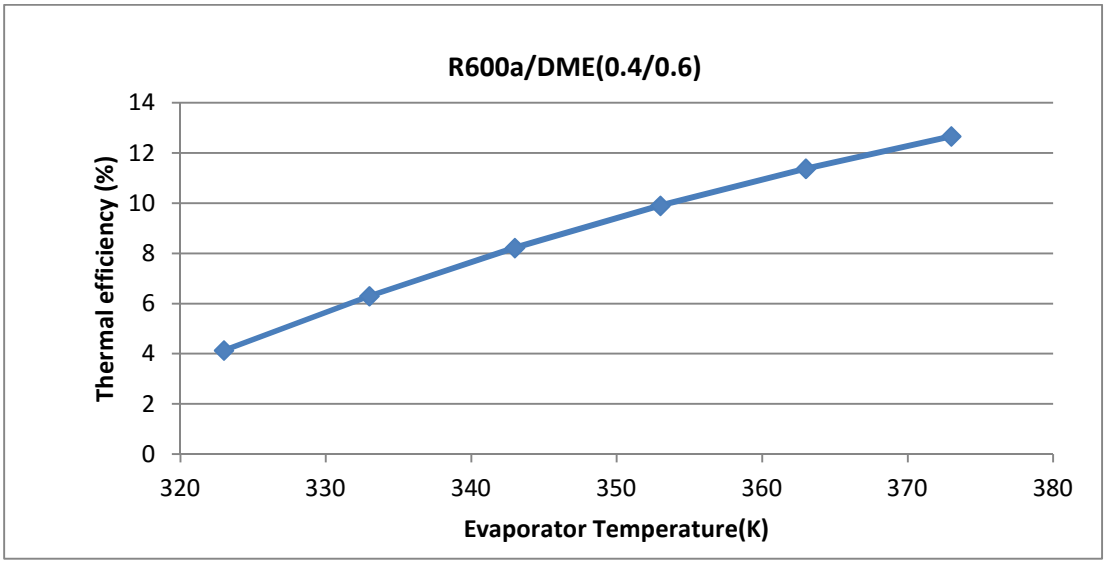

Fig.4.10 Variation of thermal efficiency with temperature of mixture R600a/DME (0.4/0.6) at inlet to evaporator

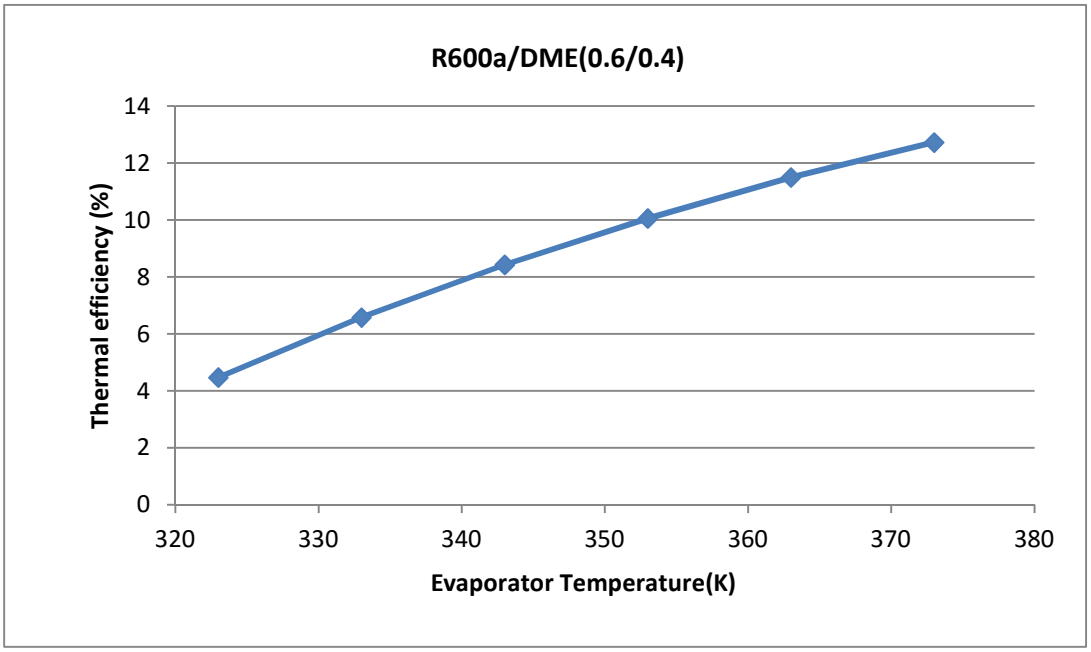

Fig.4.11 Variation of thermal efficiency with temperature of mixture R600a/DME (0.6/0.4) at inlet to evaporator

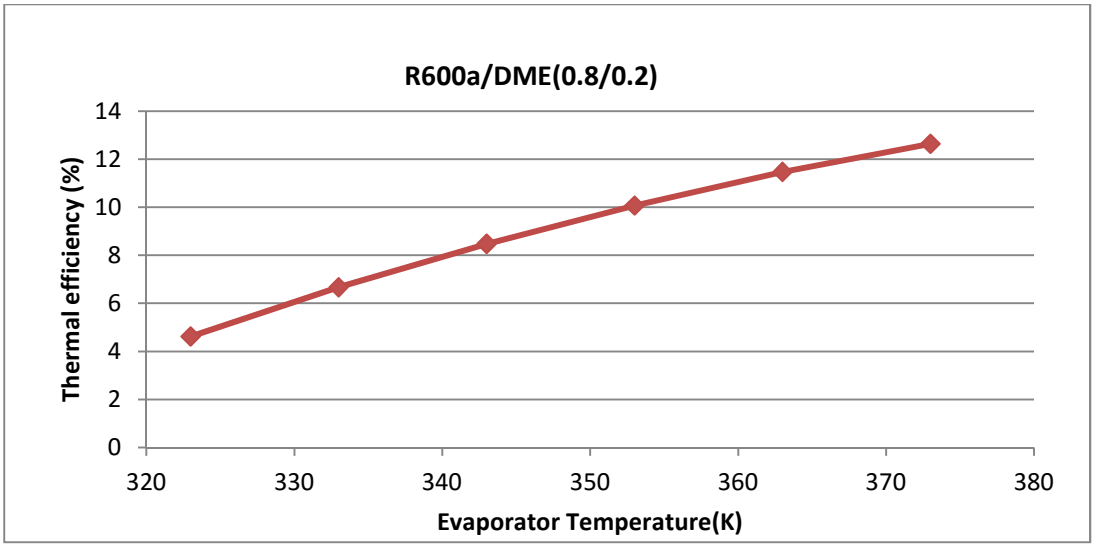

Fig.4.12 Variation of thermal efficiency with temperature of mixture R600a/DME (0.8/0.2) at inlet to evaporator

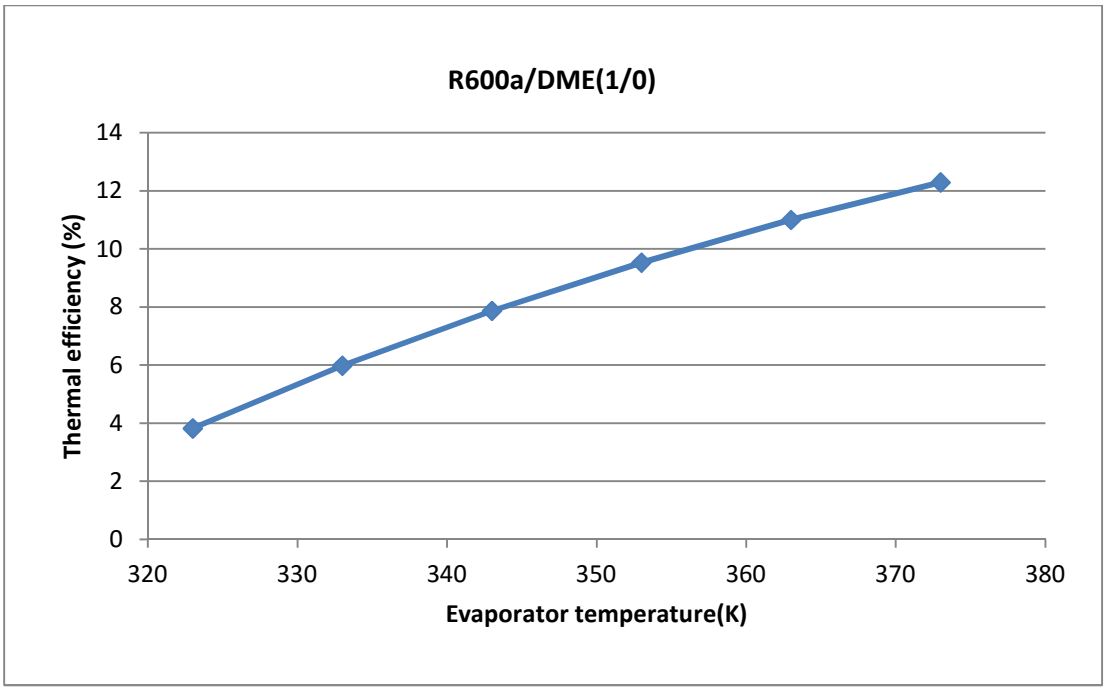

Fig.4.13 Variation of thermal efficiency with temperature of mixture R600a/DME (1/0) at inlet to evaporator

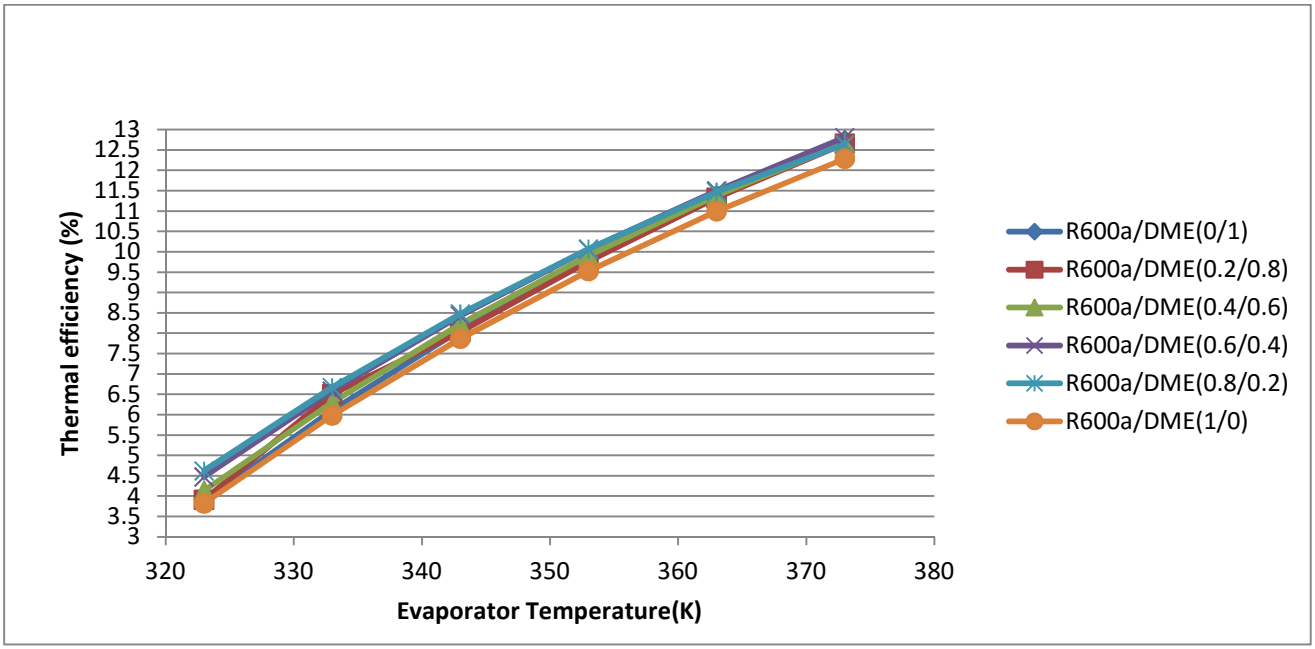

Fig.4.14 Comparison of variation of thermal efficiency with temperature at inlet to the evaporator of mixture R600a/DME for different proportions

Table4. Comparison of thermal efficiency with different inlet temperature to evaporator for each proportion of mixture of R600a/DME

Inlet temperature To evaporator(K)	**Thermal efficiency (%)**					
	Proportions of mixture of R600a/DME					
	0/1	**0.2/0.4**	**0.4/0.6**	**0.6/0.4**	**0.8/0.2**	**1/0**
323	3.888	3.935	4.135	4.472	4.621	3.822
333	6.108	6.168	6.3	6.581	6.671	5.983
343	8.085	8.128	8.222	8.433	8.475	7.869
353	9.835	9.839	9.905	10.06	10.07	9.531
363	11.39	11.33	11.38	11.5	11.47	11
373	12.74	12.59	12.67	12.81	12.64	12.39

.

4.3 EXERGETIC EFFICIENCY

Fig.4.15 to fig.4.20 show a variation of exergetic efficiency of system against temperature of mixture (R600a/DME) at the inlet to the evaporator for six different proportions. Fig.4.21 shows comparison in exergetic efficiency for all six proportions of R600a/DME against evaporator inlet temperature. By increasing inlet temperature to evaporator, exergetic efficiency of system continuously increases upto an optimum temperature.

Amongst all selected proportions, R600a/DME (0.6/0.4) has the maximum exergetic efficiency about 54.3% corresponding to 373K inlet temperature to the evaporator. R600a/DME (0.4/0.6) has second best exergetic efficiency about 53.91% corresponding to 373K inlet temperature to the evaporator. R600a/DME (1/0) has least exergetic efficiency of system corresponding to 323K temperature of mixture at the inlet to the evaporator.

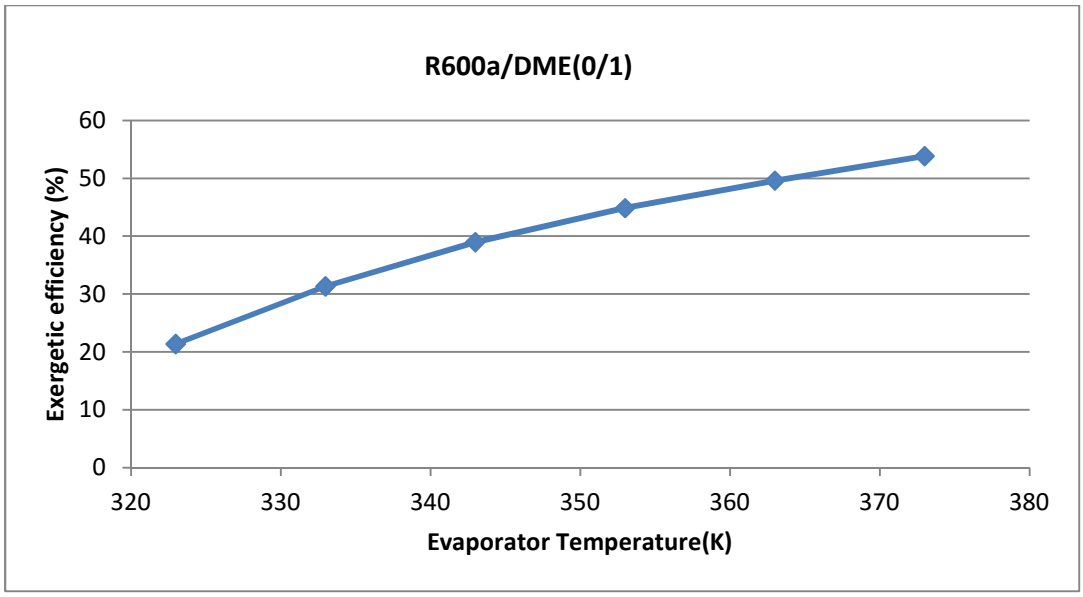

Fig.4.15 Variation of exergetic efficiency with temperature of mixture R600a/DME (0/1) at inlet to evaporator

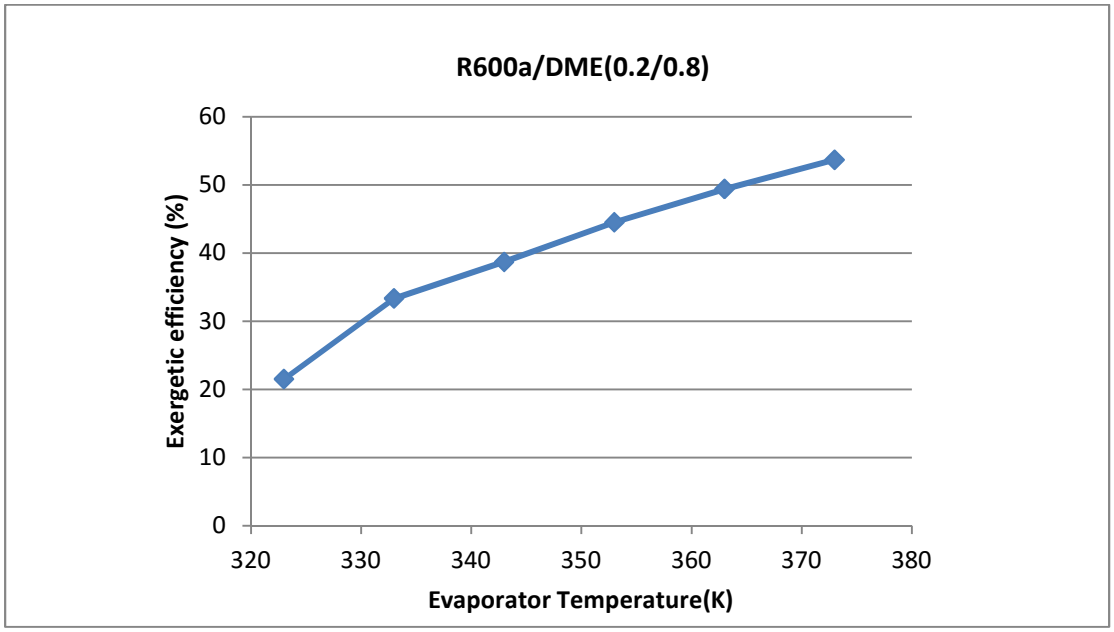

Fig.4.16 Variation of exergetic efficiency with temperature of mixture R600a/DME (0.2/0.8) at inlet to evaporator

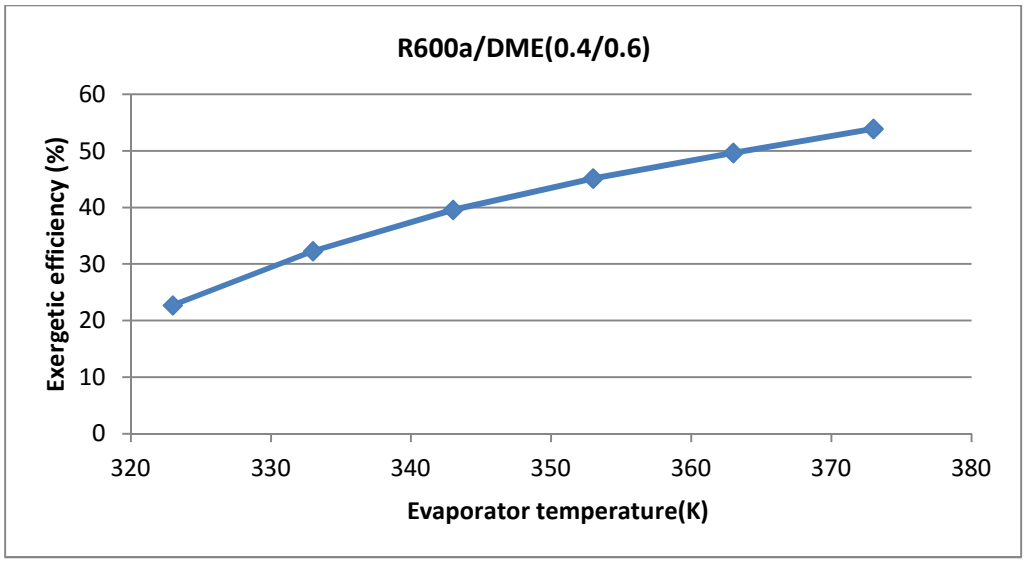

Fig.17 Variation of exergetic efficiency with temperature of mixture R600a/DME (0.4/0.6) at inlet to evaporator

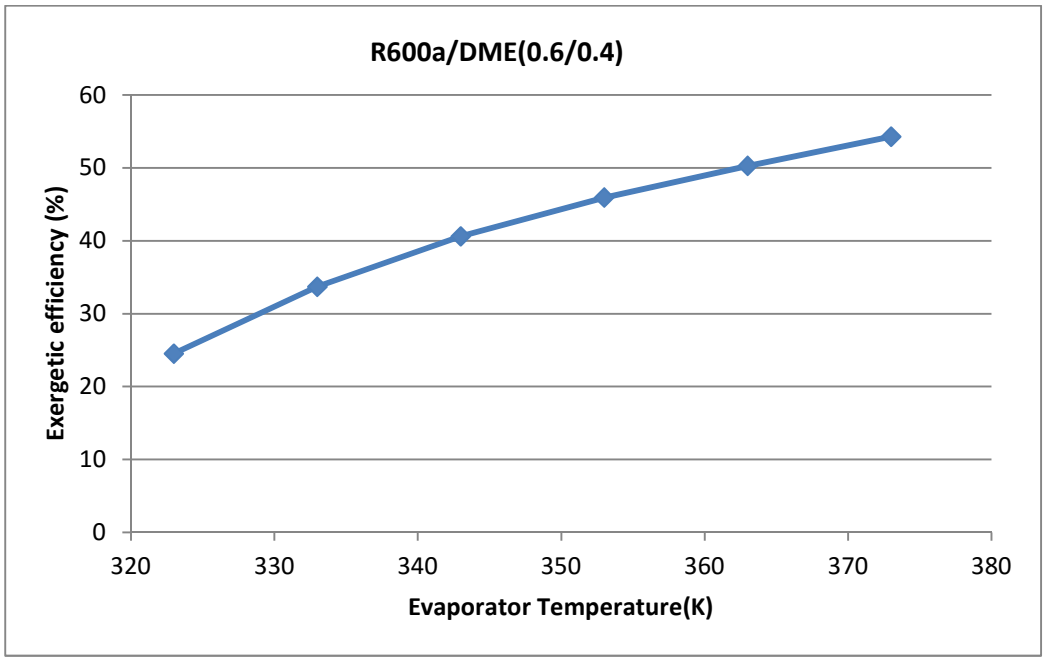

Fig.4.18 Variation of exergetic efficiency with temperature of mixture R600a/DME (0.6/0.4) at inlet to evaporator

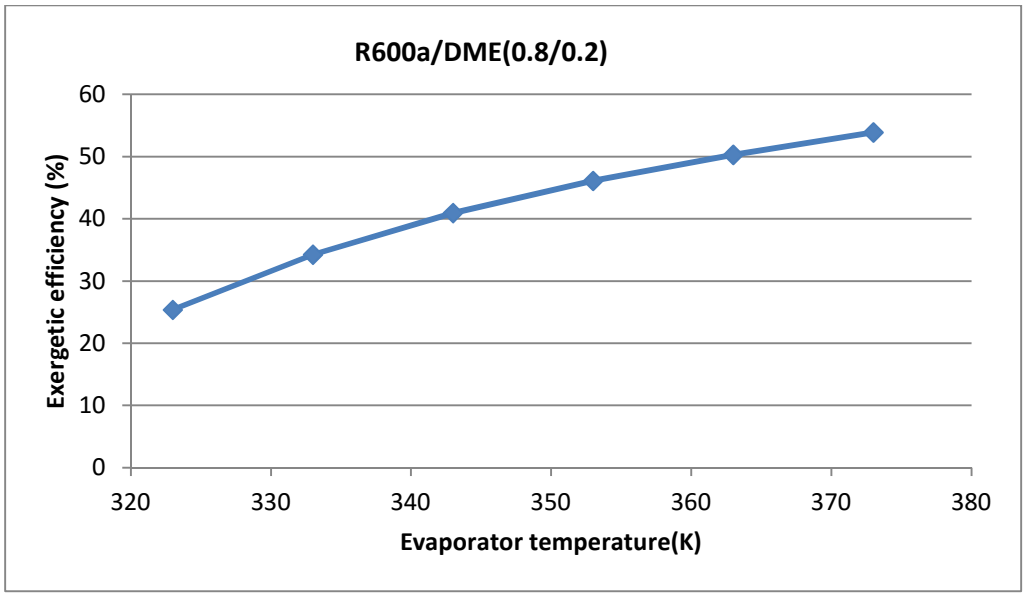

Fig.4.19 Variation of exergetic efficiency with temperature of mixture R600a/DME (0.8/0.2) at inlet to evaporator

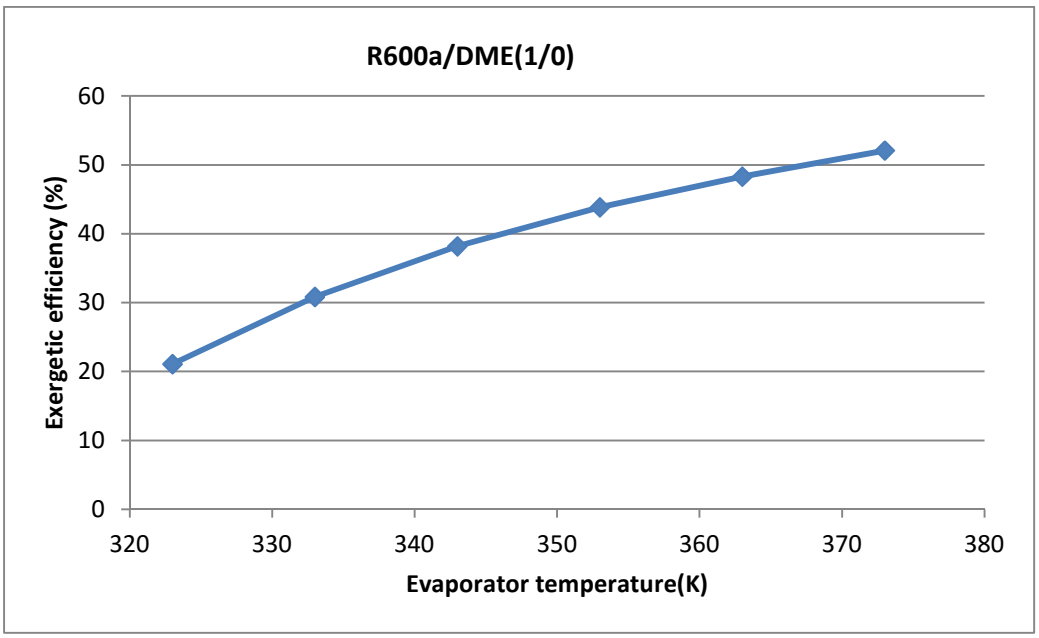

Fig.4.20 Variation of exergetic efficiency with temperature of mixture R600a/DME (1/0) at inlet to evaporator

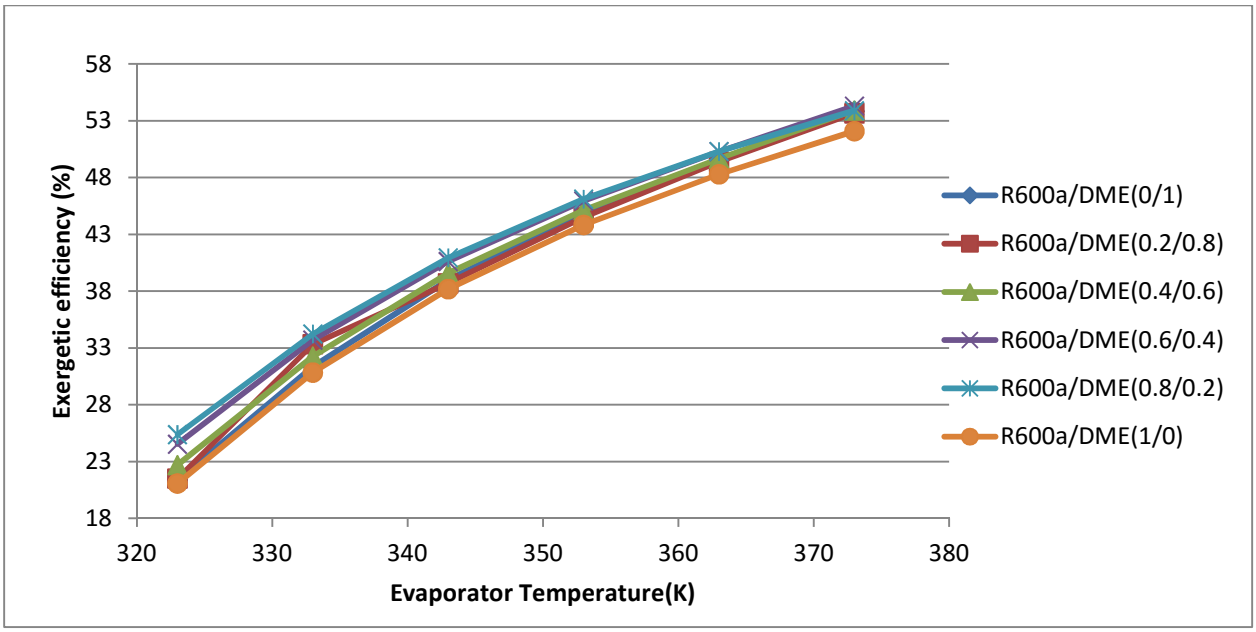

Fig.4.21 Comparison of variation of exergetic efficiency with temperature at inlet to the evaporator of mixture R600a/DME for different proportions

Table5. Comparison of exergetic efficiency with different inlet temperature to evaporator for each proportion of mixture of R600a/DME

Inlet temperature To evaporator(K)	**Exergetic efficiency (%)**					
	Proportions of mixture of R600a/DME					
	0/1	**0.2/0.4**	**0.4/0.6**	**0.6/0.4**	**0.8/0.2**	**1/0**
323	21.39	21.51	22.7	24.53	25.38	21.08
333	31.36	33.34	32.27	33.7	34.24	30.84
343	38.99	38.7	39.58	40.62	40.95	38.19
353	44.87	44.5	45.14	45.94	46.11	43.84
363	49.62	49.39	49.67	50.29	50.3	48.3
373	53.86	53.67	53.91	54.3	53.89	52.09

.

4.4 IRREVERSIBILITY

Fig.4.22 to fig.4.27 show a variation of irreversibility present in each component of system and total irreversibility present in system against mass fraction of more volatile component, which is Isobutane (R600a) for a range of inlet temperature (323K to 373K) to the evaporator.

From the mathematical analysis graphs show that total irreversibility present in the system is approximately constant for each using mass fraction of isobutane, but irreversibility present in evaporator is minimum, when we select the mass fraction of isobutane is around 0.6 and irreversibility present in condenser is maximum for same mass fraction (around 0.6) of isobutane.

If we talk about irreversibility present in pump and turbine, which is approximately constant throughout for each mass fraction of R600a.

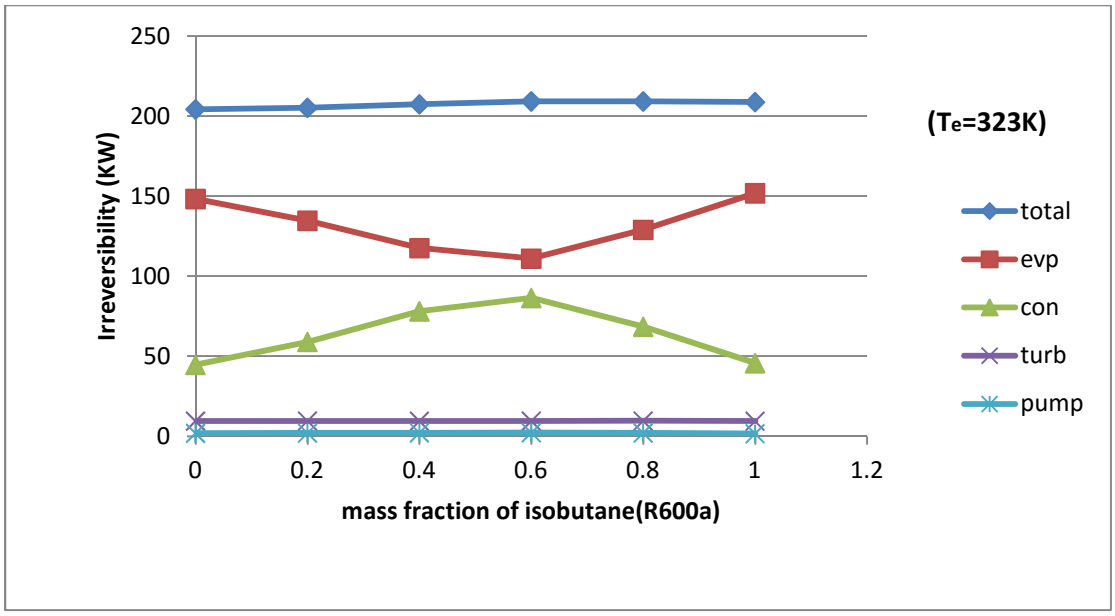

Fig.4.22 Variation of irreversibility present in system for 323K inlet temperature to evaporator against mass fraction of R600a

Table6. Irreversibility rate in each component of system for different proportions of mixture (R600a/DME) at 323K inlet temperature to evaporator

Different proportions of mixture (R600a/DME)	**Irreversibility rate (kW)**				
	Total	**Evaporator**	**Condenser**	**Turbine**	**Pump**
0/1	204.3	148.3	44.60	9.496	1.898
0.2/0.8	205.2	134.7	58.97	9.576	2.019
0.4/0.6	207.4	117.6	78.10	9.507	2.134
0.6/0.4	209.3	111	86.46	9.573	2.213
0.8/0.2	209.2	129	68.54	9.62	2.031
1/0	208.8	151.9	45.75	9.429	1.643

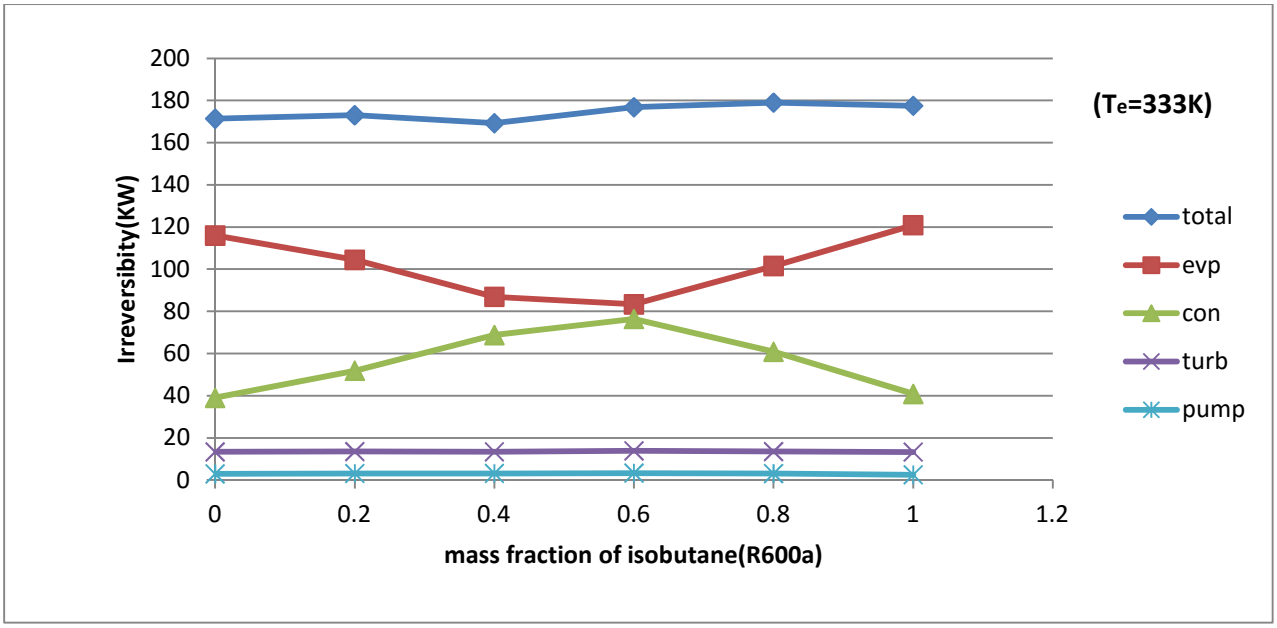

Fig.4.23 Variation of irreversibility present in system for 333K inlet temperature to evaporator against mass fraction of R600a

Table7. Irreversibility rate in each component of system for different proportions of mixture (R600a/DME) at 333K inlet temperature to evaporator

Different proportions of mixture (R600a/DME)	**Irreversibility rate (kW)**				
	Total	**Evaporator**	**condenser**	**Turbine**	**Pump**
0/1	171.4	116	39.05	13.37	2.917
0.2/0.8	173	104.4	51.88	13.52	3.140
0.4/0.6	169.2	86.92	68.78	13.39	3.143
0.6/0.4	176.8	83.32	76.4	13.83	3.297
0.8/0.2	179	101.5	60.86	13.52	3.093
1/0	177.5	120.9	40.82	13.30	2.515

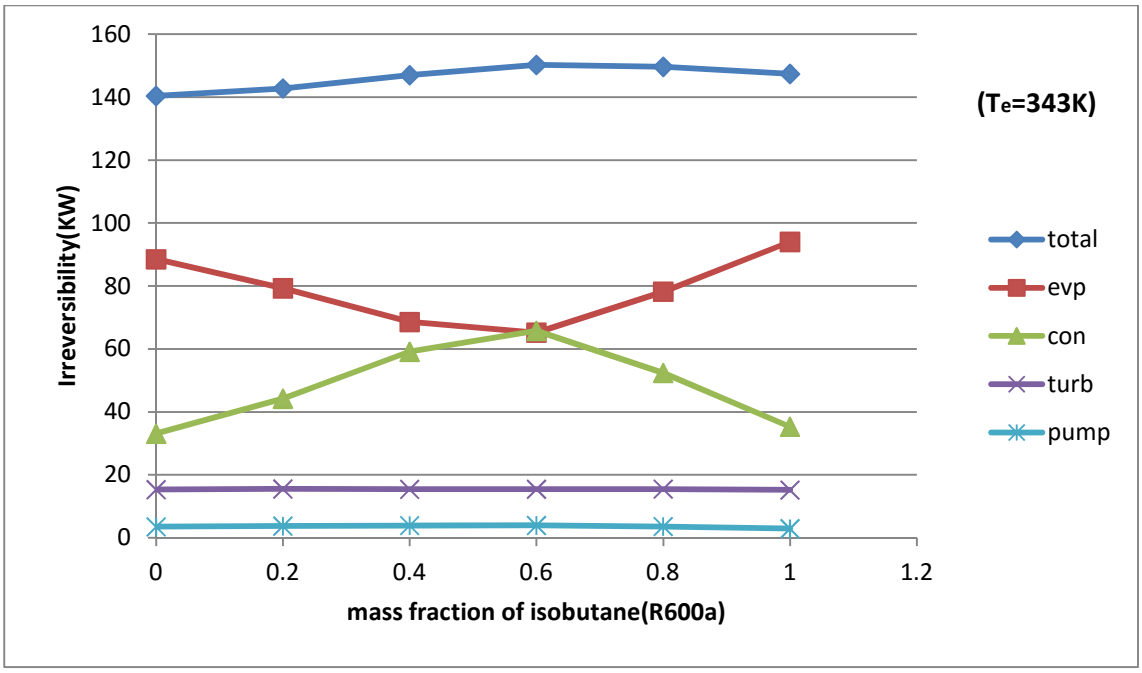

Fig.4.24 Variation of irreversibility present in system for 343K inlet temperature to evaporator against mass fraction of R600a

Table8. Irreversibility rate in each component of system for different proportions of mixture (R600a/DME) at 343K inlet temperature to evaporator

Different proportions of mixture (R600a/DME)	**Irreversibility rate (kW)**				
	Total	**Evaporator**	**condenser**	**Turbine**	**Pump**
0/1	140.4	88.52	33.1	15.33	3.495
0.2/0.8	142.8	79.29	44.23	15.51	3.726
0.4/0.6	147	68.58	59.12	15.42	3.889
0.6/0.4	150.3	65.2	65.76	15.44	3.939
0.8/0.2	149.7	78.22	52.4	15.49	3.593
1/0	147.4	94.02	35.32	15.19	2.897

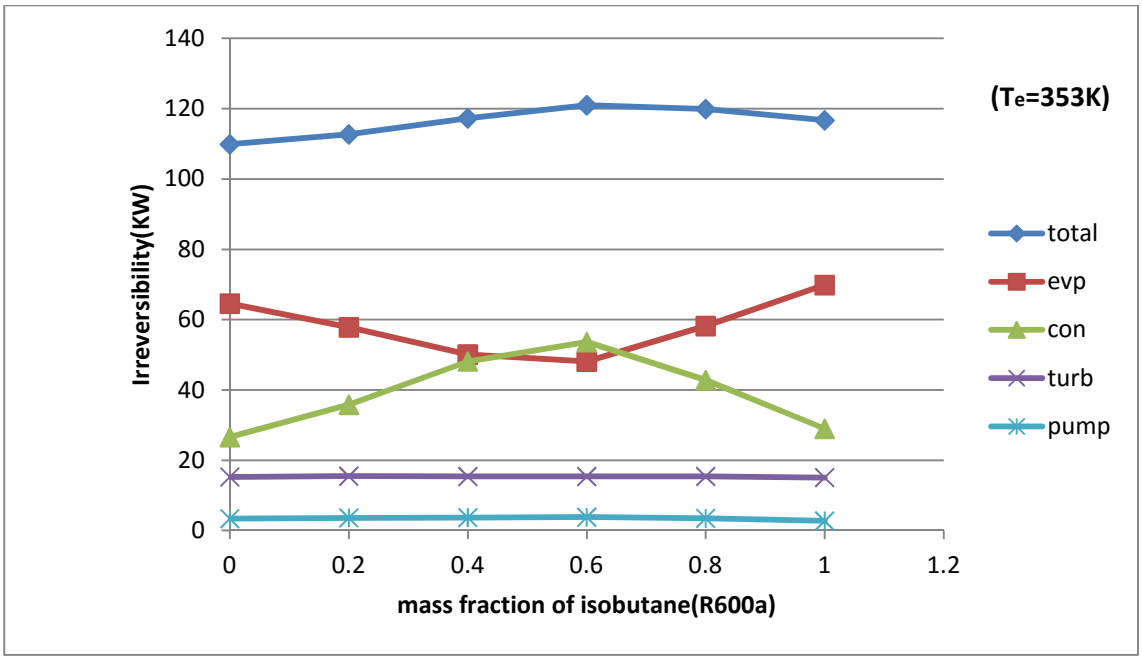

Fig. 4.25 Variation of irreversibility present in system for 353K inlet temperature to evaporator against mass fraction of R600a

Table9. Irreversibility rate in each component of system for different proportions of mixture (R600a/DME) at 353K inlet temperature to evaporator

Different proportions of mixture (R600a/DME)	**Irreversibility rate (kW)**				
	Total	**Evaporator**	**condenser**	**Turbine**	**Pump**
0/1	109.9	64.59	26.6	15.27	3.433
0.2/0.8	112.7	57.83	35.8	15.49	3.62
0.4/0.6	117.3	50.09	48.14	15.39	3.71
0.6/0.4	121	48.09	53.67	15.40	3.827
0.8/0.2	119.9	58.18	42.84	15.42	3.497
1/0	116.7	69.87	28.97	15.10	2.761

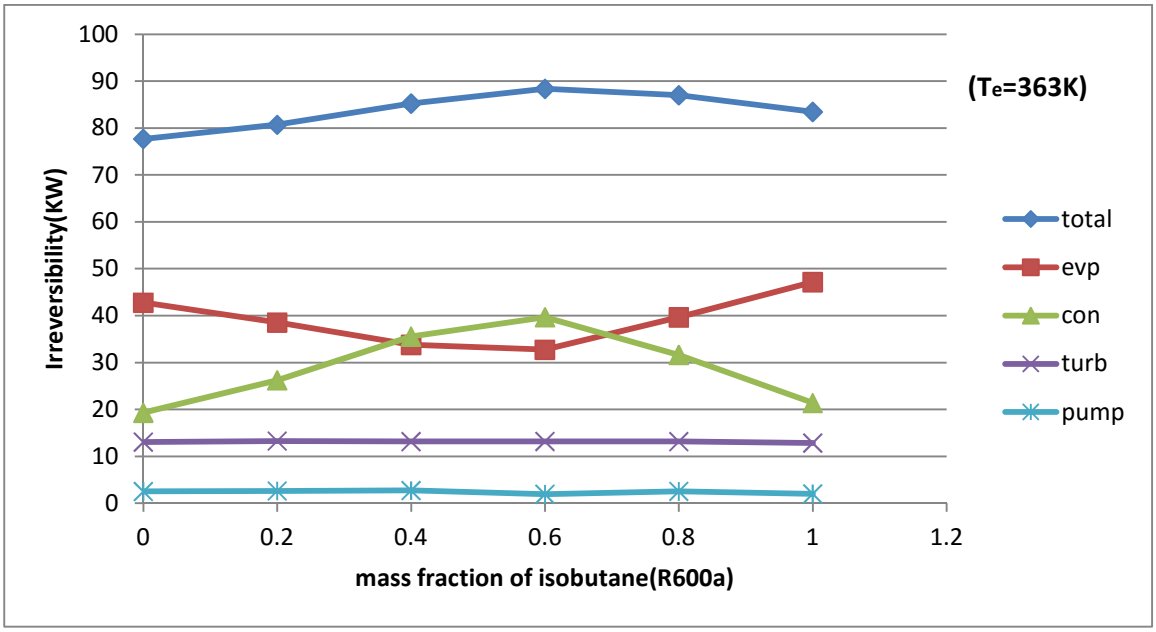

Fig. 4.26 Variation of irreversibility present in system for 363K inlet temperature to evaporator against mass fraction of R600a

Table10. Irreversibility rate in each component of system for different proportions of mixture (R600a/DME) at 363K inlet temperature to evaporator

Different proportions of mixture (R600a/DME)	**Irreversibility rate (kW)**				
	Total	**Evaporator**	**condenser**	**Turbine**	**Pump**
0/1	77.69	42.77	19.32	13.07	2.532
0.2/0.8	80.7	38.54	26.24	13.28	2.636
0.4/0.6	85.23	33.78	35.56	13.17	2.721
0.6/0.4	88.35	32.74	39.68	13.19	1.932
0.8/0.2	87.01	39.64	31.64	13.17	2.548
1/0	83.45	47.17	21.40	12.85	2.023

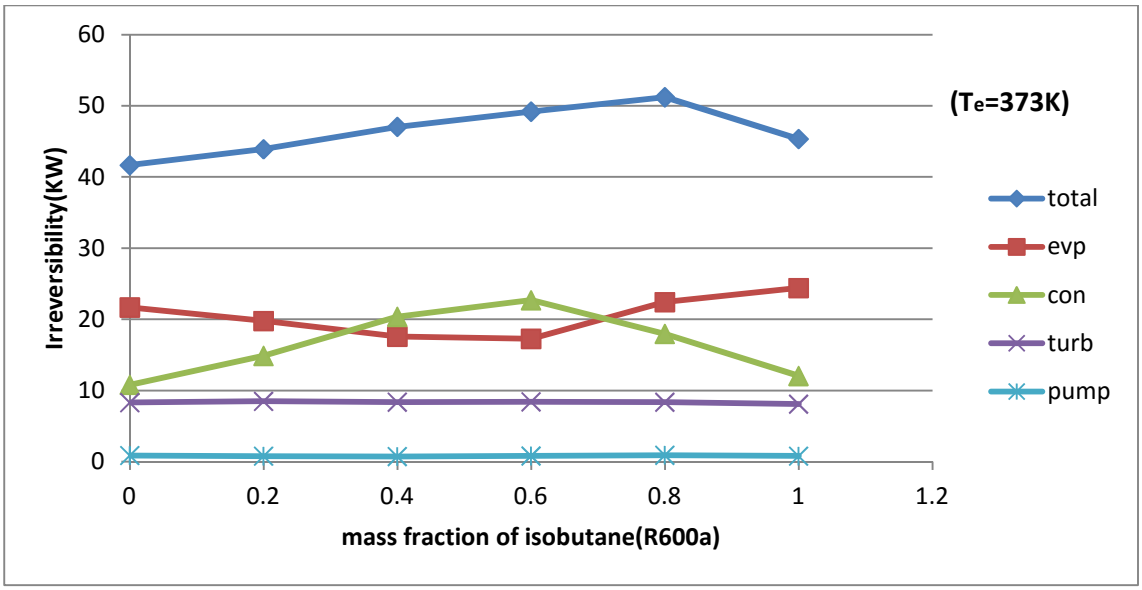

Fig.4.27 Variation of irreversibility present in system for 373K inlet temperature to evaporator against mass fraction of R600a

Table11. Irreversibility rate in each component of system for different proportions of mixture (R600a/DME) at 373K inlet temperature to evaporator

Different proportions of mixture (R600a/DME)	Irreversibility rate (kW)				
	Total	Evaporator	condenser	Turbine	Pump
0/1	41.66	21.68	10.81	8.304	0.872
0.2/0.8	43.91	19.77	14.87	8.486	0.783
0.4/0.6	47.05	17.57	20.38	8.368	0.731
0.6/0.4	49.19	17.26	22.69	8.421	0.811
0.8/0.2	51.21	22.42	17.96	8.361	0.911
1/0	45.34	24.40	12.06	8.093	0.791

4.5 MASS FLOW RATE OF MIXTURE

Here also by performing mathematical analysis, we have calculate mass flow rate of zeotropic mixture which is used in this system for producing work output.

By using software and mathematical analysis, we have found the variation of mass flow rate of zeotropic mixture against mass fraction of most volatile organic fluid, which is R600a, by draw the suitable graphs for different range of inlet temperature to the evaporator. Fig.4.28 to fig.4.33 shows a beautiful variation of mass flow rate of zeotropic mixture against mass fraction of R600a.

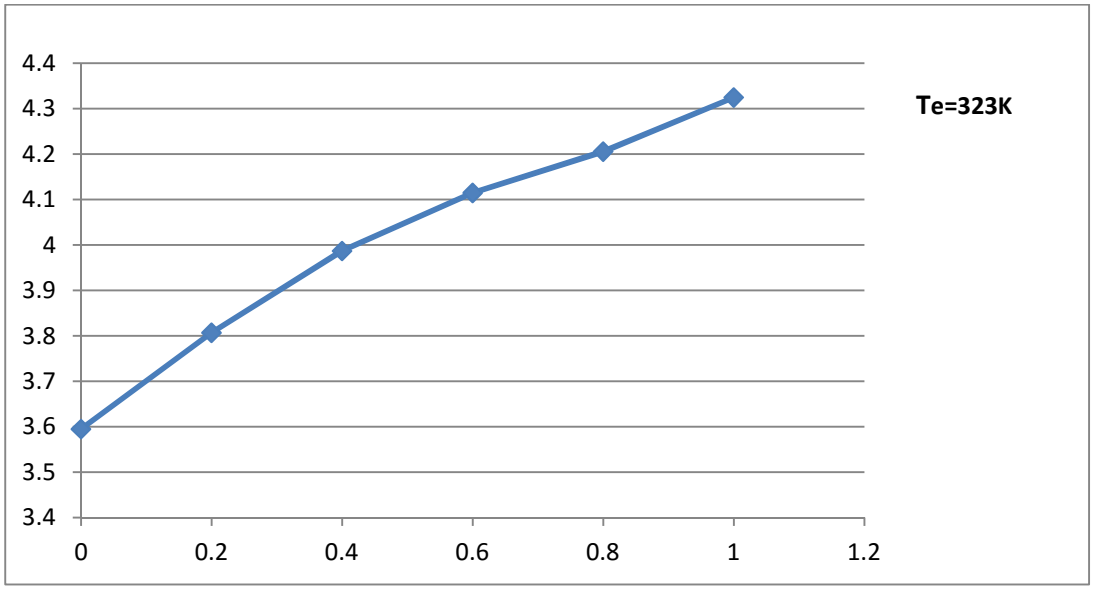

Fig.4.28 Variation of mass flow rate of mixture used for 323K inlet temperature to evaporator against mass fraction of R600a

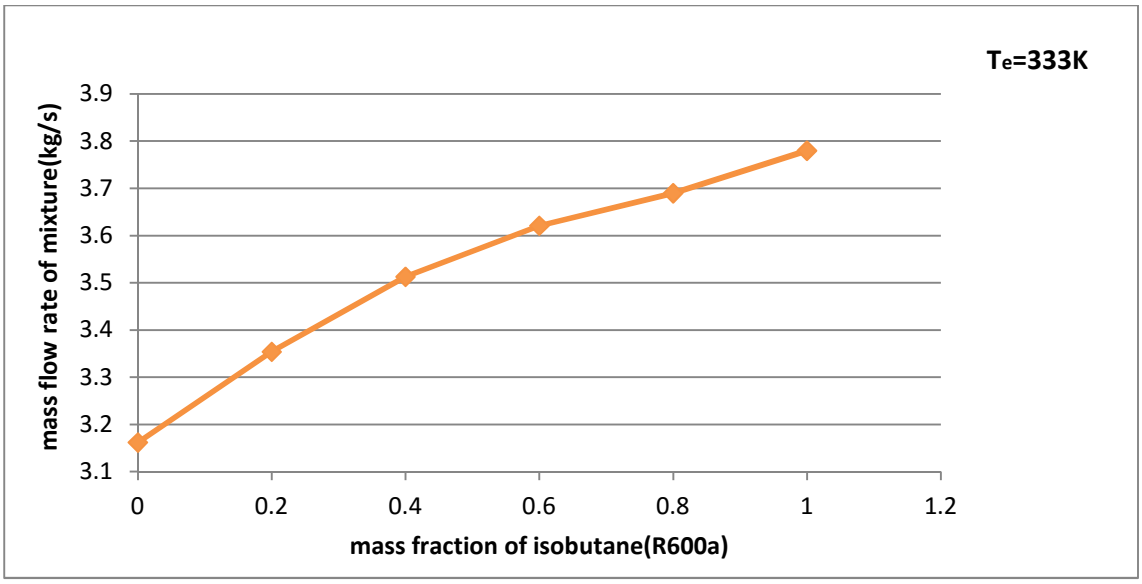

Fig.4.29 Variation of mass flow rate of mixture used for 333K inlet temperature to evaporator against mass fraction of R600a

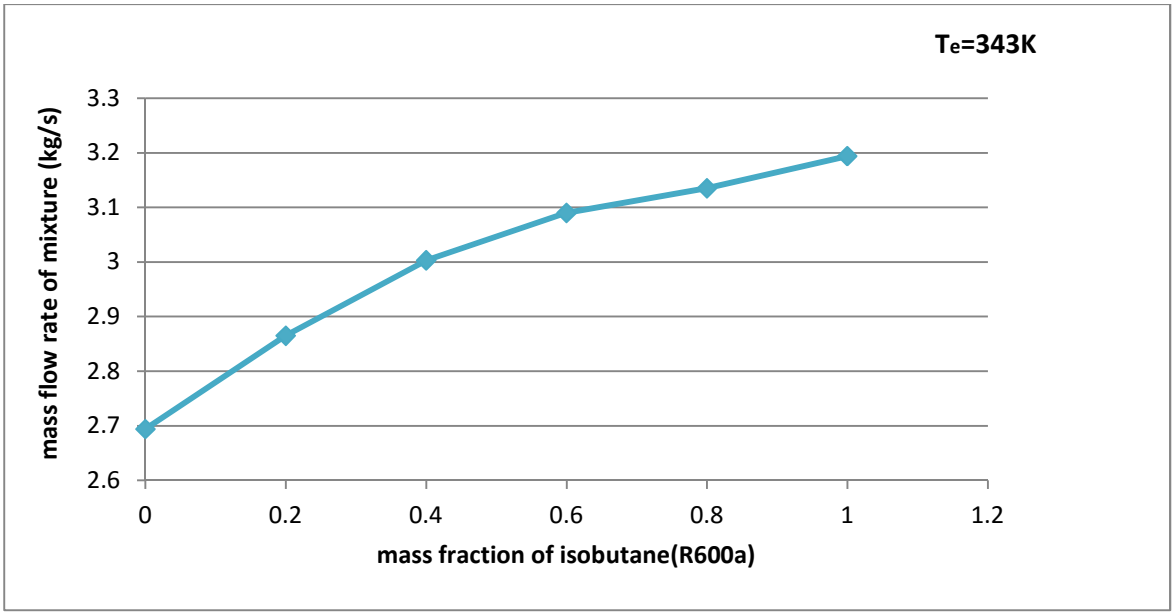

Fig.4.30 Variation of mass flow rate of mixture used for 343K inlet temperature to evaporator against mass fraction of R600a

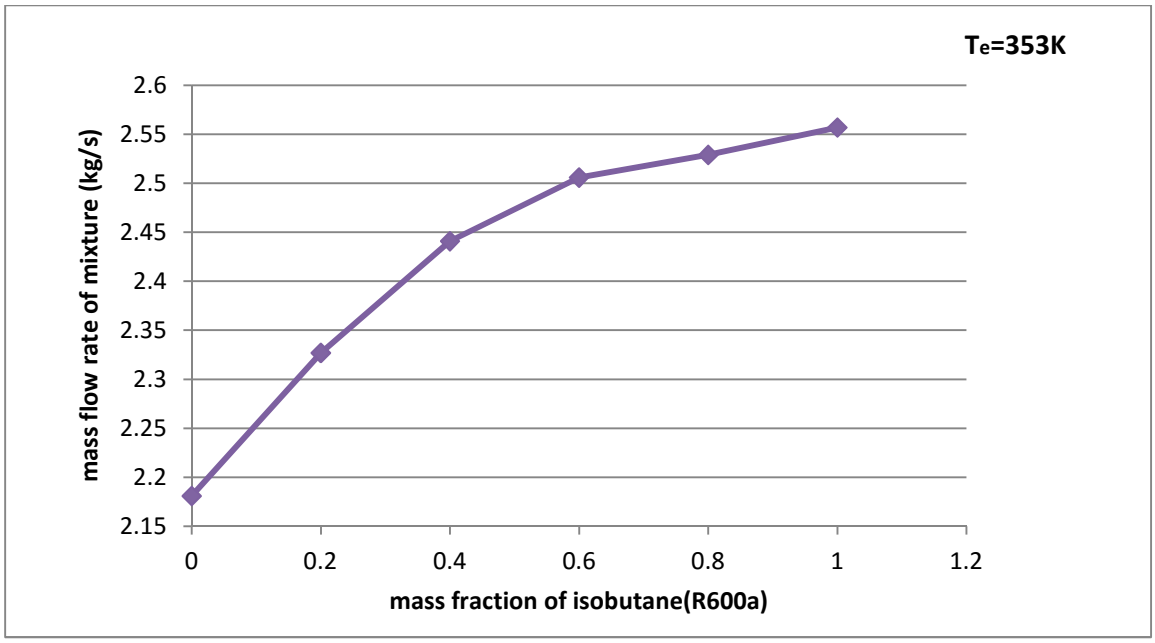

Fig.4.31 Variation of mass flow rate of mixture used for 353K inlet temperature to evaporator against mass fraction of R600a

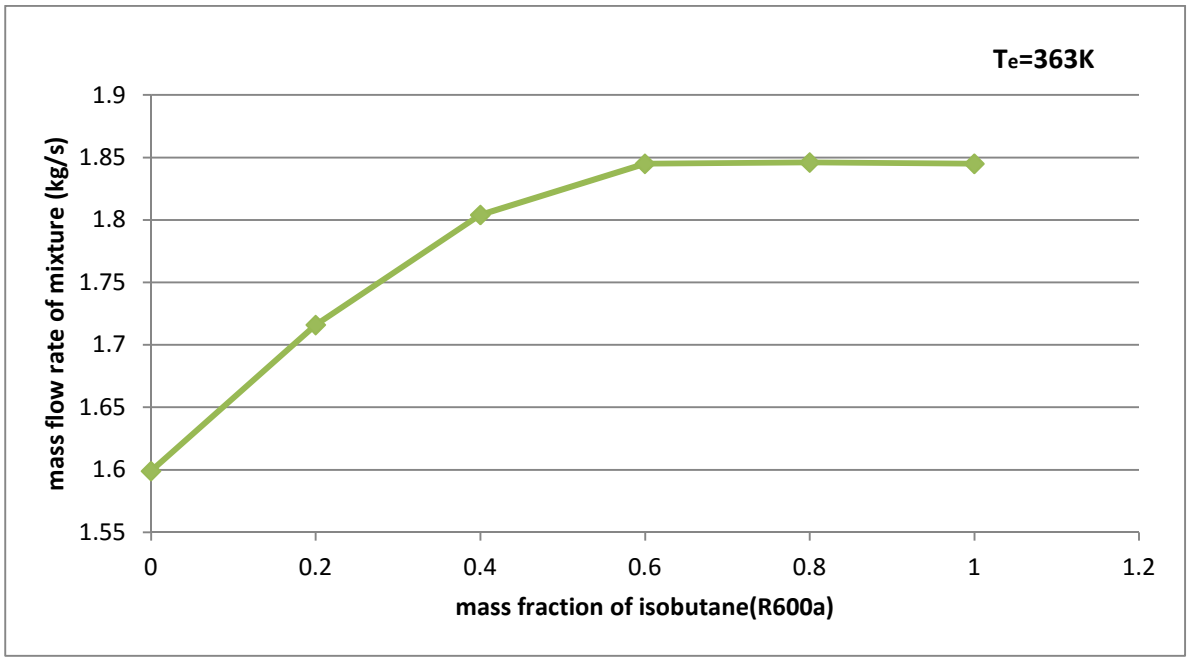

Fig.4.32 Variation of mass flow rate of mixture used for 363K inlet temperature to evaporator against mass fraction of R600a

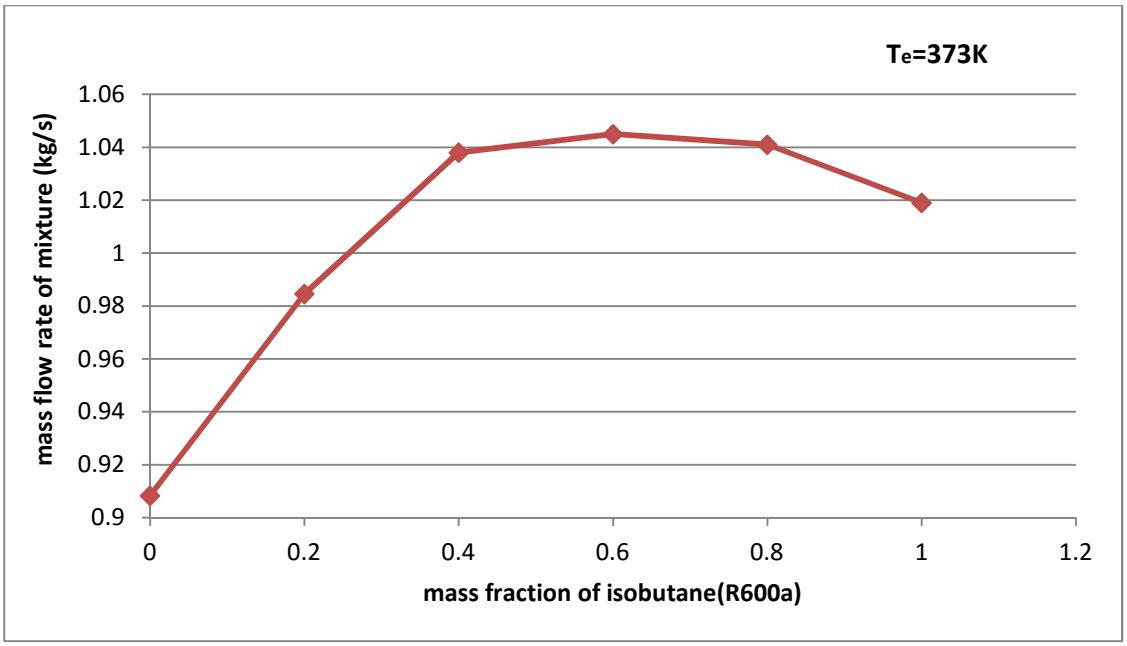

Fig.4.33 Variation of mass flow rate of mixture used for 373K inlet temperature to evaporator against mass fraction of R600a

Table12. Variation in mass flow rate of mixture with different proportions of mixture for various inlet temperatures to evaporator

Different proportions of mixture (R600a/DME)	**Mass flow rate of mixture (kg/s)**					
	Various inlet temperatures to evaporator (K)					
	323	**333**	**343**	**353**	**363**	**373**
0/1	3.59	3.16	2.69	2.18	1.599	0.908
0.2/0.8	3.80	3.35	2.86	2.32	1.716	0.984
0.4/0.6	3.98	3.51	3.00	2.44	1.804	1.038
0.6/0.4	4.11	3.62	3.09	2.50	1.845	1.045
0.8/0.2	4.20	3.69	3.13	2.52	1.846	1.041
1/0	4.32	3.78	3.19	2.55	1.845	1.019

CHAPTER-5
CONCLUSIONS

In this thesis, an extensive First law (energy) and Second law (exergy) analysis of geothermal organic Rankine cycle using zeotropic mixture of R600a and DME in different mass proportions are presented. In this work many graphs showing variation in thermal efficiency, exergetic efficiency and net work output of system against temperature of mixture at inlet to evaporator are also presented.

Conclusions of this thesis are summarised as follows:

1. Thermal efficiency (First law efficiency) and Exergetic efficiency (Second law efficiency) of organic rankine cycle increases with temperature of mixture at inlet to the evaporator.

2. Mixture ratio R600a/DME (0.8/0.2) gives maximum net work output corresponding to 343K inlet temperature to evaporator.

3. Irreversibility present in evaporator is minimum at optimal mass proportion of mixture R600a/DME (0.6/0.4) and irreversibility in condenser is maximum corresponding to mass proportion R600a/DME (.6/.4).

4. By this analysis, it is found that total irreversibility present in system is approximately constant for each mass ratio of mixture.

5. By this analysis, also found that mass flow rate of mixture goes on increasing with inlet temperature to evaporator due to which size of turbine increases. Therefore R600a/DME (0.6/0.4) can select as optimal mixing ratio for each inlet temperature to evaporator.

R600a/DME (0.8/0.2) can be considered as best option among six different mass proportions because this mass ratio gives the maximum net work output corresponding to an optimal evaporating temperature. Amongst all selected proportions, R600a/DME (0.6/0.4) has maximum thermal efficiency corresponding to 373K inlet temperature to evaporator and R600a/DME (0.6/0.4) has maximum exergetic efficiency corresponding to 373K inlet temperature to evaporator also.

CHAPTER-6

SCOPE FOR FUTURE WORK

1. Further investigation should be carried out of regenerative and superheated ORC by using this zeotropic mixture.
2. Actual organic Rankine cycle should be studied for this system by considering pressure drop in condenser and evaporator.
3. By varying the evaporator and condenser pressure of system, the First law and Second law analysis should be studied.

REFERENCES

[1] http://www.kgraenergy.com/technical/organic-rankine-cycle-history.

[2] http://theenergylibrary.com

[3] http://www.clean-energy-ideas.com/geothermal_power.html.

[4] Angelino G, Paliano P. Multicomponent working fluids for organic Rankine cycles (ORCs). Energy 1998;23,449–63.

[5] Kaila and Krishna, 1992; Gupta, 1981; Ravi Shanker, 1988, G.S.I., 1987; G.S.I.. 1991.

[6] (Giggenbach, 1976; Giggenbach et al., 1983; Nevada and Rao, 1991; Chandrasekharam et al., 1989; 1992; 1996. Chandrasekharam and Antu, 1995; Chandrasekharam and Jayaprakash, 1996; Chandrasekharam et al., 1997).

[7] Heberle F, Preibinger M, Brüggemann D. Zeotropic mixtures as working fluids in Organic Rankine Cycles for low-enthalpy geothermal resources. Renew Energy 2012;37:364–70.

[8] Baik YJ, Kim M, Chang KC, Lee YS, Yoon HK. Power enhancement potential of a mixture transcritical cycle for a low-temperature geothermal power generation. Energy 2012;47:70–6.

[9] Liu Q, Duan YY, Yang Z. Effect of condensation temperature glide on the performance of organic Rankine cycles with zeotropic mixture working fluids. Appl Energy 2014;115:394–404.

[10] Papadopoulos AI, Stijepovic M, Linke P. On the systematic design and selection of optimal working fluids for Organic Rankine Cycles. Appl. Therm. Eng 2010; 30:760-9.

[11] Demuth. O. Analyses of mixed hydrocarbon binary thermodynamic cycles for moderate temperature geothermal resources. Intersociety energy conversion engineering conference, Atlanta (USA); 1981.

[12] Heberle F, Brüggemann D. Exergy based fluid selection for a geothermal Organic Rankine Cycle for combined heat and power generation. Appl Therm Eng 2010;30:1326–32.

[13] Kim K, Ko H, Kim S. Analysis of cogeneration system in series circuit based on regenerative Organic Rankine Cycle. Adv Mater Res 2012;505:519–23.

[14] A. Borsukiewicz-Gozdur, W. Nowak, Comparative analysis of natural and synthetic refrigerants in application to low temperature Clausius-Rankine cycle, Energy 32 (04) (2007) 344-352.

[15] Habka M, Ajib S. Determination and evaluation of the operation characteristics for two configurations of combined heat and power systems depending on the heating plant parameters in low-temperature geothermal applications. Energy Convers Manage December 2013;76:996–1008.

[16] Guo T, Wang HX, Zhang SJ. Fluids and parameters optimization for a novel cogeneration system driven by low-temperature geothermal sources. Energy 2011;36:2639–49.

[17] T.C. Hung, S.K. Wang, C.H. Kuo, B.S. Pei, K.F. Tsai, A study of organic working fluids on system efficiency of an ORC using low-grade energy sources, Energy 35 (2010) 1403–1411.

[18] B.F. Tchanche, G. Papadakis, G. Lambrinos, A. Frangoudakis, Fluid selection for a low temperature solar organic Rankine cycle, Appl. Therm. Eng. 29 (2009) 2468–2476.

[19] F. Heberle, M. Preibinger, D. Brüggemann, Zeotropic mixtures as working fluids in organic Rankine cycles for low-enthalpy geothermal resources, Renew. Energy 37 (2012) 364–370.

[20] T. Deethayat, T. Kiatsirriroat, Reduction of Irreversibilities in organic Rankine cycle by non azeotropic working fluid, in: Proceedings of the STISWB V Conference, LuangPrabang, Lao PDR 2013, p. 55.

[21] J.K. Wang, L. Zhao, X.D. Wang, A comparative study of pure and zeotropic mixtures in low temperature solar Rankine cycle, Appl. Energy 87 (2010) 3366–3373.

[22] Fiaschi D, Tempesti D, Manfrida G, Di Rosa D. Absorption heat transformer (AHT) as a way to enhance low enthalpy geothermal resources. In: Proceeding of ECOS (2012) the 25th international conference. Perugia, Italy; June 26–29 2012.

[23] Gozdur A, Nowak W. Comparative analysis of natural and synthetic refrigerants in application to low temperature Clausius–Rankine Cycle. Chair of Heat Engineering, al. Piasto'w 19, 70-310 Szczecin, Poland; 31 October 2005.

[24] Li T, Zhu J, Zhang W. Comparative analysis of series and parallel geothermal systems combined power, heat and oil recovery in oilfield. Appl Therm Eng 2013;50:1132–41.

[25] Tempesti D, Fiaschi D, Gabuzzini F. Thermo-economic assessment of a micro CHP system fuelled by geothermal and solar energy. In: Proceeding of ECOS (2012) the 25th international conference. Perugia, Italy; June 26–29 2012.

[26] Khennich M, Galanis N, Sorin M. Comparison of combined heat and powersystems using an Organic Rankine Cycle and a low-temperature heat source. Int J Low-Carbon Technol 2013.

[27] Mago PJ, Srinivasan KK, Chamra LM, Somayaji C.An examination of exergy destruction in organic rankine cycle. Int J Energy Res 2008;32(10):926–38. http://dx.doi.org/10.1002/er.1406.

[28] Roy J, Mishra M, Misra A. Parametric optimization and performance analysis of a waste heat recovery system using organic rankine cycle. Energy 2010;35(12):5049–62. http://dx.doi.org/10.1016/j.energy.2010.08.013.

[29] Heberle F, Preißinger M, Brüggemann D. Zeotropic mixtures as working fluids in organic rankine cycles for low-enthalpy geothermal resources. Renew Energy 2012;37(1):364–70. http://dx.doi.org/10.1016/j.renene.2011.06.044.

[30] Ho T, Mao SS, Greif R. Comparison of the organic flash cycle (OFC) to other advanced vapor cycles for intermediate and high temperature waste heat reclamation and solar thermal energy. Energy 2012;42(1):213–23. http:// Fig. 3dx.doi.org/10.1016/j.energy.2012.03.067.

[31] Liu Q, Duan Y, Yang Z. Effect of condensation temperature glide on the performance of organic Rankine cycles with zeotropic mixture working fluids. Appl Energy 2014;115:394–404.

[32] Yang K, Zhang H, Wang Z, Zhang J, Yang F, Wang E, et al. Study of zeotropic mixtures of ORC (organic Rankine cycle) under engine various operating conditions. Energy 2013;58:494–510.
[33] Wang XD, Zhao L. Analysis of zeotropic mixtures used in low-temperature solar Rankine cycles for power generation. Sol Energy 2009;83:605–13.

[34] Garg P, Kumar P, Srinivasan K, Dutta P. Evaluation of carbon dioxide blends with isopentane and propane as working fluids for organic Rankine cycles. Appl Therm Eng 2013;52:439–48. Garg P, Kumar P, Srinivasan K, Dutta P. Evaluation of isopentane, R-245fa and their mixtures as working fluids for organic Rankine cycles. Appl Therm Eng 2013;51:292–300.
[35] Chys M, van den Broek M, Vanslambrouck B, De Paepe M. Potential of zeotropic mixtures as working fluids in organic Rankine cycles. Energy 2012;44:623–32.

[36] Venkatarathnam G, Mokashi G, Murthy SS. Occurrence of pinch points in condensers and evaporators for zeotropic refrigerant mixtures. Int J Refrig 1996;19(6):361–8.

[37] Chen HJ et al. A supercritical Rankine cycle using zeotropic mixture working fluids for the conversion of low-grade heat into power. Energy 2011;36(1):549–55.

[38] Saleh B, Koglbauer G, Wendland M, Fischer J. Working fluids for low temperature organic Rankine cycles. Energy 2007;32:1210-21.
[39] Tchanche B, Papadakis G, Lambrinos G, Frangoudakis A. Fluid selection for a low temperature solar organic Rankine cycle. Appl Therm Eng 2009;29:2468-76.

[40] Papadopoulos AI, Stijepovic M, Linke P. On the systematic design and selection of optimal working fluids for Organic Rankine Cycles. Appl Therm Eng 2010; 30:760-9.

[41] Bliem. C. Zeotropic mixtures of halocarbons as working fluids in binary geothermal power generation cycles. Intersociety energy conversion engineering conference, Portland (USA); 1987.

[42] Gawlik K, Hassani V. Advanced binary cycles: optimum working fluids. In: Geothermal resources council 1998, annual meeting, San Diego; 1998.

[43] Borsukiewicz-Gozdur A, Nowak W. Comparative analysis of natural and synthetic refrigerants in application to low temperature Clausius-Rankine cycle, Energy ECOS 05. In: Eighteenth international conference on efficiency, cost, optimization, simulation, and environmental impact of energy systems e ECOS 05. 32; 2007,344-352.

[44] A.A. Lakew, O. Bolland, Working fluids for low-temperature heat source, Appl. Therm. Eng. 30 (10) (2010) 1262-1268.

[45] Per Lundqvist, Working fluids for Organic Rankine Cycle.

[46]Bahaa S, Koglbauer G, Wendland M, Fischer J. Working fluids for low temperature organic Rankine Cycles. Energy 2007;32(7):1210–21.

[47] http://www.mcquay.com/mcquaybiz/literature/lit_ch_wc/AppGuide/AG31-006.pdf

[48] M. Calm, G. C. Hourahan (2011). Physical, Safety and Environmental data for current and alternative Refrigerants, ICR 2011, August 21 – 26 – Prague, Czech Republic

[49] F. Heberle*, M. Preißinger and D. Brüggemann. Zeotropic mixtures as working fluids in Organic Rankine Cycles for low-enthalpy,geothermal resources, Renewable Energy 37 (2012) 364-370.

[50] Z. Kang , Jialing Zhu , Xinli Lu ,Tailu Li , Xiujie Wu . Parametric optimization and performance analysis of zeotropic mixtures for an organic Rankine cycle driven by low-medium temperature geothermal fluids, Applied Thermal Engineering 89 (2015) 323-331.

[51] https://www.ocf.berkeley.edu/~hyl/me114/Chapter%2013%20Solutions.doc.

APPENDIX

COMPUTER PROGRAMME

Energy and Exergy analysis of organic rankine cycle:

```
T_ci=293
T_co=303
C_p=4.31
m_2=5
T_0=298
T_in=393
P_1=.77653
h_1=140.38
V_1=(1/645.11)
s_8=1.7526
s_1=.50211
h_8=525.52
P_2=1.1397
T_4=323
h_4=178.61
h_5=538.30
s_5=1.7350
C_pl=2.6032
s_4=.62147
ETA_t=.85
ETA_p=.75


DELTAT_pp=10
T_pp=T_4+DELTAT_pp

W_t=m_1*(h_5-h_7)
W_p=m_1*(h_3-h_1)
Q_evp=m_1*(h_5-h_3)
ETA_ther=W_net/Q_evp
W_net=W_t-W_p

m_1*(h_5-h_4)=m_2*C_p*(T_in-T_pp)
h_7=h_5-(ETA_t*(h_5-h_6))
V_1*(P_2-P_1)=h_2-h_1
h_3=h_1+((h_2-h_1)/ETA_p)

I_evp=m_1*T_0*(s_5-s_3-(h_5-h_3)/T_mevp)
I_con=m_1*T_0*(s_1-s_7-(h_1-h_7)/T_mcon)
I_t=m_1*T_0*(s_7-s_5)
I_p=m_1*T_0*(s_1-s_3)
I_total=I_evp+I_con+I_t+I_p
ETA_exer=W_net/(W_net+I_total)

s_5=s_6
T_mevp=(T_in+T_pp)/2
T_mcon=(T_ci+T_co)/2
s_7=s_1+(x_2*(s_8-s_1))
```

h_3=h_4-(C_pl*(T_4-T_3))
s_3=s_4-(C_pl*LN(T_4/T_3))
s_6=s_1+(x_1*(s_8-s_1))
h_6=h_1+(x_1*(h_8-h_1))
h_7=h_1+(x_2*(h_8-h_1))